DELFT UNIVERSITY OF TECHNOLOGY

Faculty of Mechanical, Maritime and Materials Engineering
Biomechanical Engineering Department

MSc. Thesis:

Horizontal Semicircular Canal Orientation and the 3-D Vestibulo-Ocular Reflex

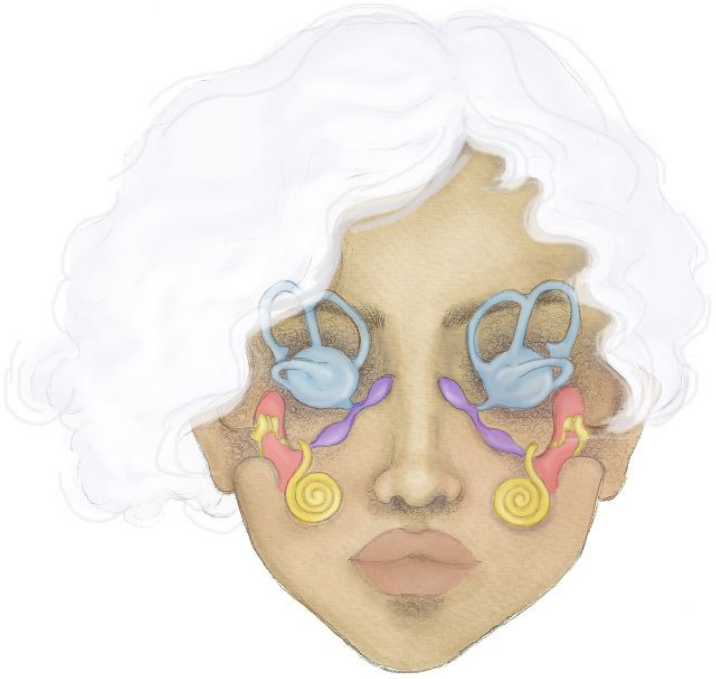

by

Lorraine Lauwerends

Supervisors:
Dr. Ir. R. Happee
Prof. Dr. J. van der Steen
Dr. Ir. J.J.M. Pel

August 2015

Information

Title:
Horizontal Semicircular Canal Orientation and the 3-D Vestibulo-Ocular Reflex

Type of report:
Master of Science Thesis

Author:
Lorraine J. Lauwerends

Student Number:
1327496

Institute:
Delft University of Technology
Faculty of Mechanical, Maritime and Materials Engineering
Department of Biomechanical Engineering
Master Biomedical Engineering

Board of Examiners:
Prof. Dr. Ir. P.P. Jonker (3mE, BMechE)
Dr. Ir. R. Happee (3mE, BMechE)
Prof. Dr. J. van der Steen (Neuroscience, EMC)
Dr. Ir. J.J.M. Pel (Neuroscience, EMC)

DELFT UNIVERSITY OF TECHNOLOGY

Abstract

Faculty of Mechanical, Maritime and Materials Engineering
Biomechanical Engineering Department

Master of Science

by Lorraine Lauwerends

Goal. The three-dimensional vestibulo-ocular reflex (3-D VOR) is responsible for the maintenance of stable vision through generating compensatory eye movements in response to head movements. The main functional components of the 3-D VOR are the semicircular canals. The anatomy of the three canals is complicated, requiring the definition of several natural coordinate systems in order to assess the canals' functionality. Most notably, the horizontal canals form a significant angle (approx. 25°) with respect to the earth-horizontal (E-H) while the head is upright. The goal of this study was to determine the influence of head pitch orientation on the quality of the VOR, and thus to identify the 3-D VOR dependence on canal anatomy and orientation.

Methods. Eight healthy upright seated subjects underwent whole-body sinusoidal and transient stimulation delivered by a six degree of freedom (6-DOF) motion platform. Small-amplitude sinusoidal oscillation was delivered around the yaw axis and axes in the horizontal plane between roll and pitch at increments of 22.5°. Transients were delivered in yaw, roll and pitch and in the vertical canal planes. This sequence of stimuli was repeated for the subject with his/her head in three different initial positions: upright, pitched nose down 16° and 25°, aligning the horizontal canal prime direction and maximum response direction with the E-H, respectively. 3-D scleral search coils were used for the recording of eye movements.

Results. For sinusoidal stimulation around axes in the horizontal plane, a decline in gain and an increase in misalignment were found for increasing downward head pitch, in the light as well as in darkness. All component gains had lower values in darkness than in light. For vertical axis rotation, this decrease in gain and increase in misalignment was also present, except for the torsion component which increased with both upward and downward (from upright) pitch. Transient stimulation yielded overall lower gains than sinusoidal stimulation. No significant differences between the different head pitch orientations were found for vertical axis stimulation. For transients around axes in the horizontal plane however, the horizontal component gain increased with increasing nose-down pitch, while overall the vertical component decreased.

Conclusions. The incongruence between the mathematically modeled coordinate systems of the semicircular canals and the obtained results in terms of gain and misalignment, suggests the contribution of other mechanisms to the 3-D VOR. The gravity-induced otolith-mediated VOR is likely to have an additional effect with the head pitched. The inhibitory effect of the otolith-mediated gravity vector on the torsional eye position is a possible explanation for the reduction in gain for sinusoidal rotation around axes in the horizontal plane. The opposite is seen during transient stimulation, which could be attributed to the otolith organs' low-pass behaviour.

Contents

Chapter 1

Introduction

One of the functions of the vestibular system is the maintenance of stable vision, by means of the vestibulo-ocular reflex (VOR). The VOR in 3-D generates compensatory and orienting eye movements in response to head rotations. It does so ideally with a magnitude equal to that of the head rotation, in the opposite direction of the head movement, and about an axis colinear with the head rotation axis. The vestibular system contains the otolith organs and the semicircular canals, which encode linear acceleration and head rotation, respectively.
The functional components of the VOR are the semicircular canals and the six extraocular muscles, which are arranged such that the eyes can turn around arbitrary axes[1]. In principle, each extraocular muscle is stimulated by one semicircular canal pair[2]. However, due to canals not being perfectly orthogonal[3], other extraocular muscles are also stimulated, albeit to lesser degrees. It is the semicircular canals' orientations which determine the canals' response to head rotation and, consecutively, the ability of the brain to interpret those movements. A peculiarity in the canals' orientation is the significant frontally upward inclination of the horizontal semicircular canals with respect to the earth-horizontal, while the head is held in the naturally upright position. In his study pondering the possibility of using the horizontal canals as a proxy to estimate head postures, de Beer was among the first to note that the direction of this angle was unique in humans, and presumed that it must be of functional and/or biological significance [4].

1.1 Semicircular Canal Coordinate Systems

There are three natural coordinate systems of the semicircular canals: the anatomical canal planes, the maximum response directions and the prime directions (see Figure 1.1). The canals are generally curved rather than exactly planar, but the anatomical canal vectors

are found by plane fitting to the anatomical center data and subsequent weighting with the inverse of the cross-sectional area squared. A single semicircular canal undergoes maximal stimulation when rotated in its plane, and will be minimally affected when rotation takes place in a plane perpendicular to that of the canal. The anatomical canal vectors are not equal to the coordinate system with which 3-D angular head movements can be decomposed. It was however found that the maximum response and anatomical vectors were nearly equivalent (see Figure 1.1), differing by an average of 2.27±1.79° for the horizontal canals [5] [6]. The third natural coordinate system of the semicircular canals is that of the prime directions [7]. This coordinate system is defined as the rotation axes that maintain a large response in a single canal while reducing the response of the sister canals to a "null" for all practical purposes. According to measurements by Cox et al.[8], the mean value and significance of deviation from 0° of the angle between the horizontal canal normal and its prime direction in humans, is 9.79 ± 3.37°, with P<0.001. Rotation in the anatomical canal plane generates the maximal response in a single canal, however it does not shut off a response in the other two canals. Single canal activation on the other hand is analogous to rotations about prime directions, making them the most likely coordinate frame used by the central neurons to separate 3-D rotations into three separate rotational components[9].

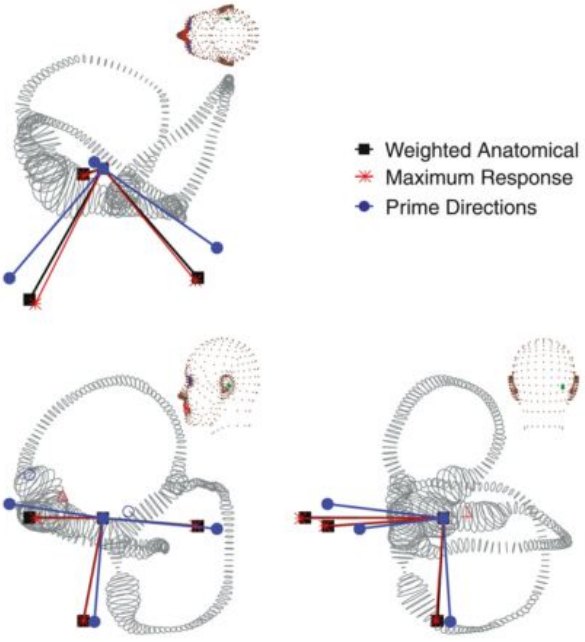

FIGURE 1.1: *Orthographic projections of vectors along the anatomical canal plane normals, maximum response directions and prime directions. Anatomical and maximum response directions are closely aligned, while prime directions don't align with either for all canals[10].*

1.2 Upward Inclination Horizontal Canals

It has been noticed early on that the human orientation of the horizontal semicircular canal is unusual when compared to other mammals. When in a normal, upright position, the horizontal canal planes form a significant angle of approximately 30°[4][3][6] with the earth horizontal, such that they presumably do not function at their maximum efficiency. The orientation of the horizontal semicircular canals has been used to determine skull orientations (how animals hold their head) in studies of non-avian dinosaurs[11]. In this field of study, the horizontal canal pitch orientation is used as a reference system to estimate how the animals held their heads, either during rest or when alert. In contrast to humans, most mammals evidently hold their heads positioned such that their horizontal canal planes are aligned with the earth-horizontal, which seems logically advantageous. For humans to achieve this orientation, they would have to bend their heads downwards, looking on to the ground at a point one or two meters in front of them[12]. While the neutral head position in man has been studied and more or less defined[4][13], 'normal' head position in man is still worthy of speculation. The head position described above, with the head tilted down significantly to align the horizontal canals with the horizon, corresponds to that commonly used when reading, walking over uneven surfaces, or to the alert stance of a boxer. The upright head position, as defined with the frontal pole of Reid's line[1] 6° above the earth-horizontal, appears unnaturally elevated, resembling a military stance[15].

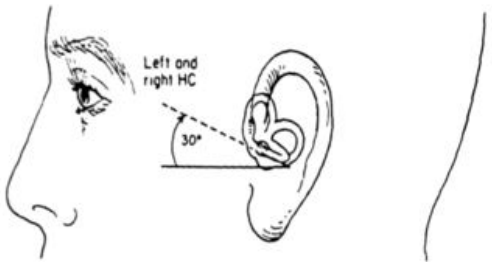

FIGURE 1.2: *Orientation of the horizontal semicircular canals.*

According to Bradshaw et al.[6], the mean horizontal semicircular canal plane is anteriorly tilted upwards by 18.8° above the Reid horizontal plane. This means that the horizontal canal maximum response direction is not aligned with the E-H when the head is held upright. In clinical testing, positioning the head slightly pitch down is part of the guidelines for the manual head impulse test (HIT) [16]. This warrants the delivery of individual head impulses in a plane more closely corresponding to the (anatomical) horizontal canal planes.

[1] An anatomical landmark which passes through the center of the external auditory canal and the inferior orbit margin[14]. The Reid stereotaxic coordinate system was used as an external reference frame for describing canal positions.

This is done to improve canal specificity, which suggests that VOR sensitivity is dependent on canal anatomy and plane orientation.

1.3 Study Goal

The distinct orientation of the horizontal semicircular canals raises questions on the functional dependency of the 3-D VOR on canal anatomy and orientation. Currently there is no literature on horizontal canal position and its functional relevance for the VOR. The goal of this study is to determine whether directional coding for the angular 3-D VOR relies entirely on the three-canal orientation, most importantly focusing on the upward inclination of the horizontal canals with respect to the E-H. Using estimates obtained through biomechanical modeling of the maximal response and prime directions of the horizontal semicircular canals from previous research[5] as a reference point, we observed the 3-D VOR in eight healthy subjects in response to 3-D whole-body rotations. Sinusoidal and transient stimuli were delivered to the subjects with their heads in three different initial head pitch positions, such that three different horizontal canal orientations could be compared:

- Upright (frontal pole of Reid axis oriented 6° above the earth-horizontal),
- Horizontal anatomical canal plane approximately aligned with the E-H (frontal pole of Reid axis oriented 25° below the E-H), and
- Horizontal canal prime direction approximately aligned with the E-H (frontal pole of Reid axis oriented 16° below the E-H).

Note that in this report the horizontal anatomical canal plane is considered interchangeable with the horizontal maximal response plane. The position of the visual target did not change during the experiment, such that gaze direction remained constant while sagittal eye-in-orbit position changed along with the different head pitch positions. The gain (ratio between eye and head velocity) and misalignment (angle between eye and head rotation axes) are considered the main determinants of VOR quality, and were systematically investigated. Assuming that the maximal response and prime directions will be reflected in the results, we predict that the composition of component gains in the 3-D VOR will vary between the different head pitch angles accordingly with the attenuation of gains by the cosine of the angle between the optical axis and plane of head rotation. As pitching the head nose-down results in a vertical axis (yaw) rotation more closely in the maximal response plane of the horizontal canals, we expect maximal horizontal component as well as 3-D vector gain under these conditions.

Chapter 2

Methods

2.1 Subjects

Eight healthy subjects participated in the experiments, aged between 18-65 years. Subjects aged 70 and older were excluded from participation beforehand, because of the high prevalence of vestibular dysfunction in that age group [17]. None of the subjects had a medical history or clinical signs of vestibular, neurological or oculomotor abnormalities. All subjects gave their written informed consent. The experimental procedure was in accordance with the Declaration of Helsinki for research involving human subjects and was approved by the Medical Ethics Committee of the Erasmus Medical Center.

2.2 Motion Platform

A motion platform (FCS-MOOG, Nieuw-Vennep, the Netherlands) capable of generating accurate movements with six degrees of freedom (6-DOF) was used to deliver the stimuli. The platform is controlled by six electro-mechanical actuators wired to a computer with dedicated control software (HostEMC). The platform motion profile is continuously monitored by position sensors placed in the actuators. These sensors have established that the device has < 0.5 mm precision for linear and $< 0.05^{\circ}$ precision for angular movements. The motion platforms high resonance frequency (> 75 Hz) prevented vibrations during stimulation ($< 0.02^{\circ}$).

To verify the accuracy of the platforms motion generation, output was measured with a dummy coil fixed in space within the magnetic field during sinusoidal stimulation. Compared with the stimulus signal sent to the platform, it was confirmed that the platform produced a nearly perfect sinusoidal stimulus. During experiments, sensors in the actuators monitored the platform motion profile, which was reconstructed and sent to the data

collection computer at a rate of 100 Hz. For precise synchronization of platform and eye movement data, a laser beam attached to the back of the platform was projected onto a small photocell at the base of a 0.8 mm pinhole (reaction time 10 μs). The output voltage of the photocell was sampled at a rate of 1 kHz. This was done simultaneously with the output data, so that the photocell signal provided a real time indicator of zero crossings of the platform motion onset with 1 ms accuracy. Matlab (Mathworks, Natick, MA) was used for the off-line analysis in which the reconstructed motion profile of the platform based on the sensor information of the actuators in the platform was precisely aligned with the onset of the platform motion as indicated by the drop in voltage of the photocell.

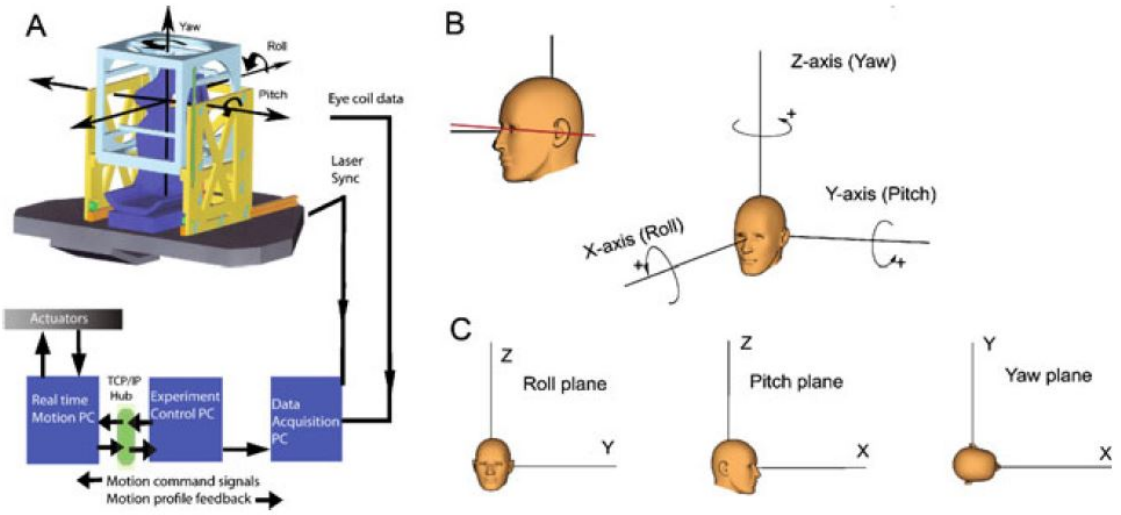

FIGURE 2.1: *1A) Schematic drawing of the 6-DOF motion platform also representing the computer hardware and signal flow for the control of platform movements and the monitoring of platform motion and eye movements. 1B) The seated subject's head orientation. In the standard (upright) orientation, Reid's line makes an angle of 6° with the earth horizontal. 1C) Rotation directions around the cardinal axes according to the right-hand rule.*

2.3 Eye Movement Recording

Eye movements were recorded with 3-D scleral search coils (Skalar, Delft, the Netherlands), utilizing a 25 kHz two field coil system based off the amplitude detection method of Robinson (Model EMP3020, Skalar Medical, Delft, the Netherlands). Coil signals were passed through an analogue low-pass filter with cutoff frequency of 500 Hz and sampled on-line and stored to hard disk at a frequency of 1000 Hz with 16-bit precision (CED system running Spike2 v6, Cambridge Electronic Design, Cambridge).

A head-fixed, right-handed coordinate system was used for the definition of eye rotation (as in Figure 2.1C). The positive rotations were defined as follows (from the subject's point of view): leftward rotation about the Z-axis (yaw), downward rotation about the Y-axis

(pitch), rightward rotation about the X-axis (roll). Consequently, the roll, pitch and yaw planes are orthogonal to respectively the X, Y and Z rotation axis.

2.3.1 Calibration

A coil calibration session was performed prior to actual measurements, the data from which was used for the transformation of the coil voltages into Fick angles (see section 2.6). A five-point calibration pattern (a center target with four targets at 10° to its left, right, up and down) was projected on a screen located at 189 cm in front of the subject at eye level. Subjects were instructed to fixate the targets for four seconds each successively.

2.4 Experimental Protocol

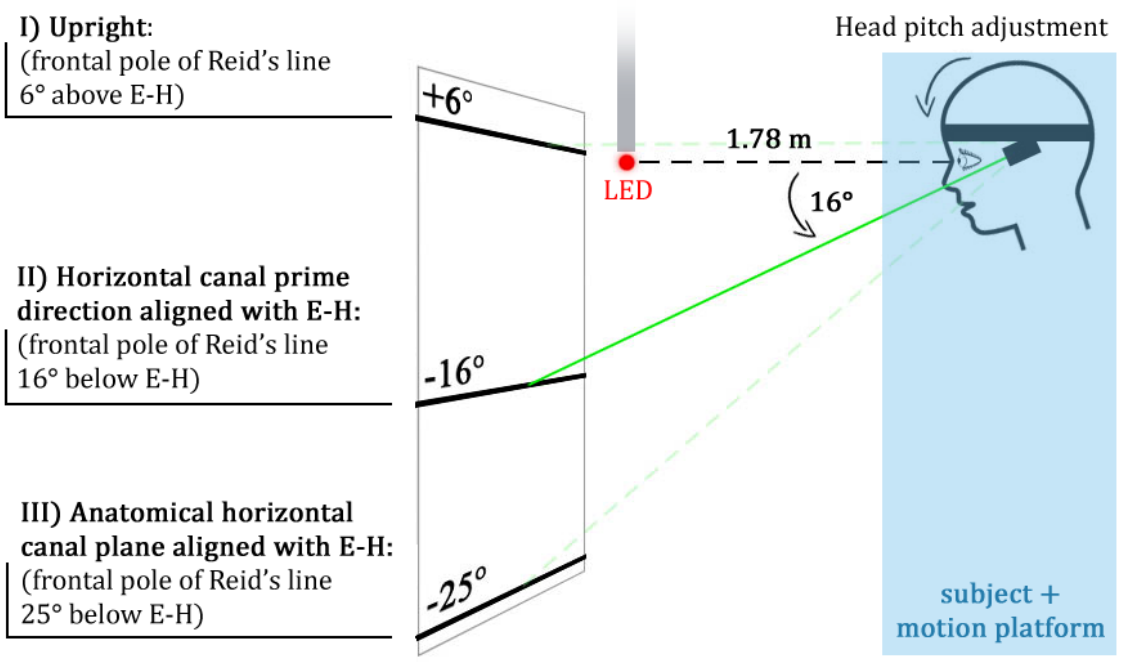

FIGURE 2.2: *Setup for adjusting head positions. The subject is seated on the motion platform in front of the ceiling-mounted visual LED-target (red dot) and a lined sheet. The three marked lines stand for the orientations of the frontal pole of Reid's line w.r.t. the E-H. The subject pitches his/her head between measurements by pointing the head-mounted laser (green line) on the lines. At each head pitch angle, the subject's gaze (dashed line) should be directed towards the fixed LED-target. In the present figure, the subject's head is in position II) Horizontal canal prime direction aligned with E-H: frontal pole of Reid's line 16° below E-H.*

Prior to the experiments, a dental impression board with the purpose of immobilizing the head was made of the subject. Subjects then took place on the platform seat and secured the four-point seat-belt. Subjects under 178 cm in height were seated on top of an additional pillow to bring their head closer into the center of the search coil frame, such that the

head was in the middle of the magnetic field, as well as in line with the platform rotation axis. At the beginning of the experiment, a laser pointer fixed to the subject's head was used to determine head pitch orientation with respect to gravity and its orientation center. The bite board containing the dental impression board was adjustable in pitch angle and towards and away from the subject. First the subject was instructed to position their head and bite board such that they felt as close as possible to straight up. In front of the subject in the platform at a distance of 189 cm hung a sheet with three lines indicating the three relevant head positions for the measurement: straight up (with Reid's line approximately at 6° above earth-horizontal (E-H)), with the horizontal canals' prime direction aligned with the E-H (with Reid's line approximately at 16° below E-H) and with the horizontal canal plane aligned with the E-H (with Reid's line approximately at 25° below E-H)(see Figure 2.2), which was also the most physically demanding position for the subject. Two control subjects were measured with their head in two positions: upright and with the head pitched nose-up 18°.

With the platform temporarily elevated to its active position, each subject manually adjusted the laser pointer, their head and the bite board to position the laser on each of the three lines consecutively (as a means of practice), ending with their head in an upright position (see Figure 2.2). After lowering the platform, the subject received tetracaine ophthalmic drops and the scleral search coils were inserted into one or both eyes, depending on the subjects' tolerance of the coils.

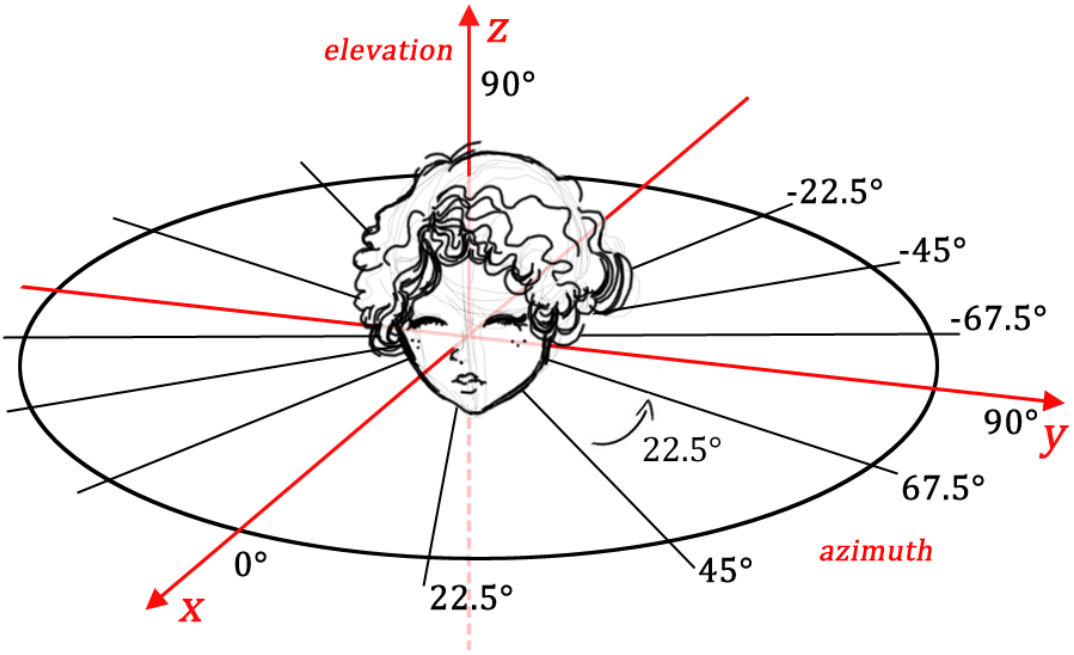

FIGURE 2.3: *All rotation axes for sinusoidal stimulation, 9 in total. The red lines denote the cardinal axes (roll, pitch and yaw) and the black lines represent the additional rotation axes in the horizontal plane, spaced apart 22.5°. For transient stimulation, only 5 rotation axes are included: the cardinal axes, and 2 axes in between roll and pitch, spaced apart 45°. Rotation axes in the horizontal plane are described by their degrees azimuth, and the vertical rotation axis (yaw) by its elevation. Also see Figure 2.1.*

Whole body transient and sinusoidal rotations were delivered around the vertical, inter-aural and naso-occipital axes rendering yaw, pitch and roll rotation respectively. Additional axes in the horizontal plane were also included (see Figure 2.3). This set of whole-body rotations was repeated for the three above mentioned head positions in the following order: upright, horizontal canal plane aligned with E-H, and horizontal canal's prime direction aligned with E-H. Altogether, the test takes around 35 minutes to complete, which is within the time in which the scleral search coils are tolerable. An overview of all experimental variations is shown in Figure 2.4 below.

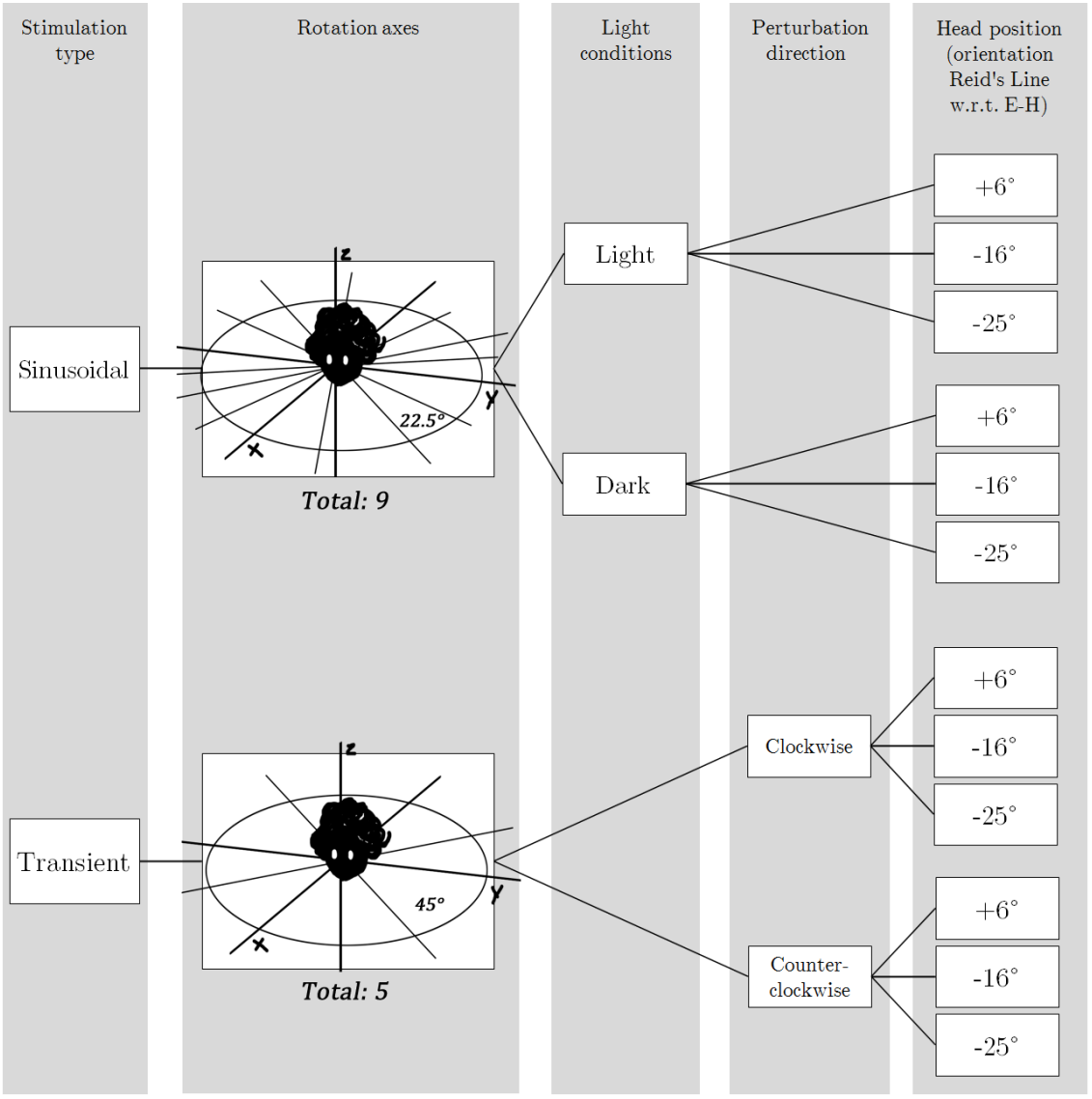

FIGURE 2.4: *Tree diagram of all experimental variations (with the exception of the controls). Head position is defined as the angle between the frontal pole of Reid's line with the Earth-horizontal (E-H). i.e. different head pitch positions.*

2.5 Motion Stimuli

2.5.1 *Sinusoidal Stimulation*

Subjects underwent sinusoidal rotation around the rostro-caudal or earth-vertical axis (yaw), and around axes equally distributed in the horizontal plane between interaural (pitch), and nasooccipital (roll). Two of these rotation axes (45° and -45° azimuth) cause rotation approximately in the plane of the vertical semicircular canals. The orientation of the horizontal stimulus axes was incremented in steps of 22.5° azimuth at zero elevation.

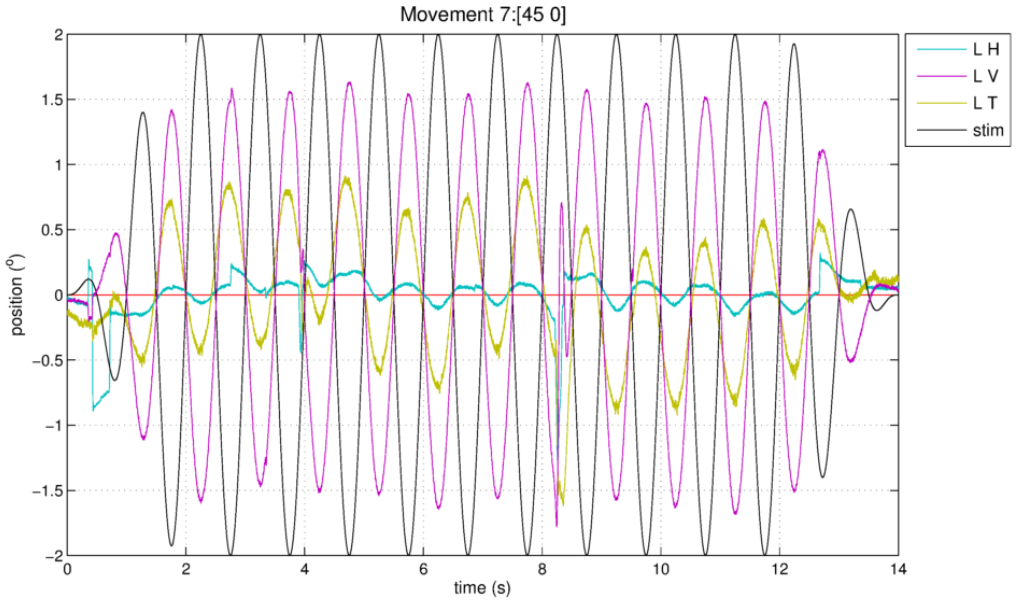

FIGURE 2.5: *Eye movements during sinusoidal stimulation in the light around an axis between roll and pitch (45° azimuth), thus predominantly consisting of a torsion and vertical component. Left eye movement components are shown together with the stimulus for its entire duration.*

Stimulation frequency was 1 Hz with a total duration of 14 s, including fade-in and fade-out time of 2 s. Peak-to-peak amplitude of the rotation was 4°, resulting in peak acceleration of $80°/s^2$. Stimulation was chosen to mimic the frequency of normal activities such as walking, where the predominant frequency is 0.8 Hz with a mean amplitude of 6°[18].
The visual target was a red LED (2 mm in diameter) at eye level close to the primary position, at a distance of 177 cm. Sinusoidal stimulation was delivered during two "light" conditions for the visual target:

- **Light:** Subjects fixated the continuously lit LED in an otherwise darkened room.
- **Dark:** The LED was presented briefly (2 s) in between two stimulations when the platform was stationary. After viewing the space fixed target, the subjects were instructed to fixate its imaginary location during sinusoidal stimulation after it had been switched off just before motion onset.

2.5.2 *Transient Stimulation*

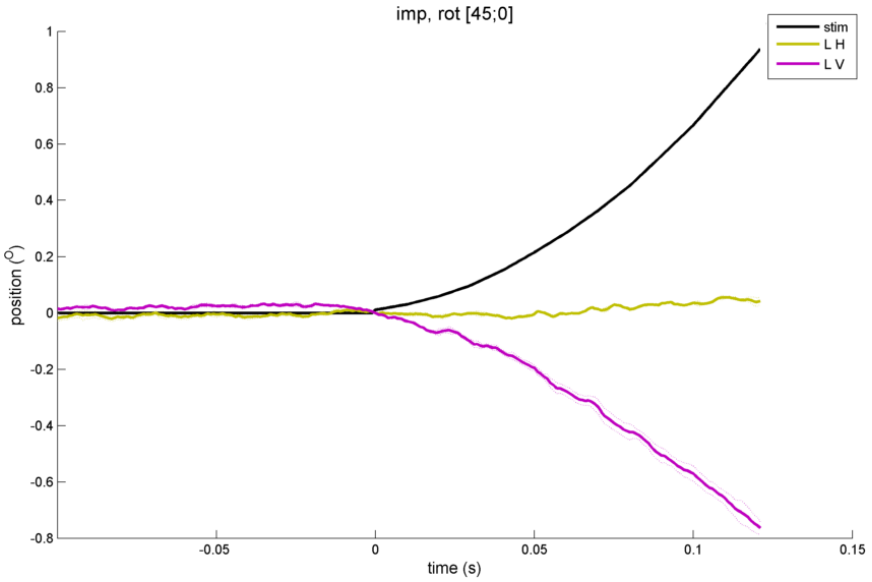

FIGURE 2.6: *Transient around an axis between roll and pitch (45° azimuth). In this figure, the black line denotes the stimulus, while the purple and green traces denote vertical and horizontal left eye movements respectively.*

Transient stimulation was included for having the possibility of measuring the VOR during the first 100 ms, during which no visual contribution is present. Subjects underwent short-duration whole body transients while viewing a visual target at eye level at a distance of 177 cm in a fully darkened environment. Transients were delivered around the earth-vertical axis (yaw), and around axes equally distributed in the horizontal plane between inter-aural (pitch), and naso-occipital (roll), with increments in steps of 45° azimuth. Rotation around each axis was repeated three times. Transients were delivered in random order, and at random motion onset timing (with intervals varying between 2.5 and 3.5 s). The transient profile was a constant acceleration of $100°/s^2$ during the first 100 ms of the transient, followed by a gradual linear decrease in acceleration. Transients are a useful addition to sinusoidal stimulation, as the time frame during which they are measured (first 100 ms) and their unpredictable onset timing rule out the contribution of nonvestibular eye movement systems (e.g. visual, anticipatory) to the response[19].

2.6 Data Analysis

Coil voltages were transformed into Fick angles, and from then on expressed as rotation vectors. For sinusoidal stimulation, saccades were discarded and rotation vector data was smoothed (see Fig. 2.7). Saccade recognition was based on velocity, duration, displacement and acceleration criteria. Smoothing was done by zero-phase with a forward and reverse

digital filter with a 50-point Gaussian window (length of 50 ms) for sinusoidal stimulation, and a 20-point Gaussian window for transients. Rotation vector data was then transformed into angular velocity (ω) to express eye movements in the velocity domain (gain). Gain is defined as the ratio between eye component peak velocity in head-fixed coordinates and platform (head) peak velocity in space-fixed coordinates, which can be written as:

$$\left|\frac{\vec{\omega}_e}{\vec{\omega}_h}\right| = \frac{\sqrt{\omega_{e,x}^2 + \omega_{e,y}^2 + \omega_{e,z}^2}}{\sqrt{\omega_{h,x}^2 + \omega_{h,y}^2 + \omega_{h,z}^2}} \tag{2.1}$$

where the eye velocity and head velocity vectors are as follows:

$$\vec{\omega}_e = \begin{pmatrix} \omega_{e,x} \\ \omega_{e,y} \\ \omega_{e,z} \end{pmatrix}, \quad \vec{\omega}_h = \begin{pmatrix} \omega_{h,x} \\ \omega_{h,y} \\ \omega_{h,z} \end{pmatrix}. \tag{2.2}$$

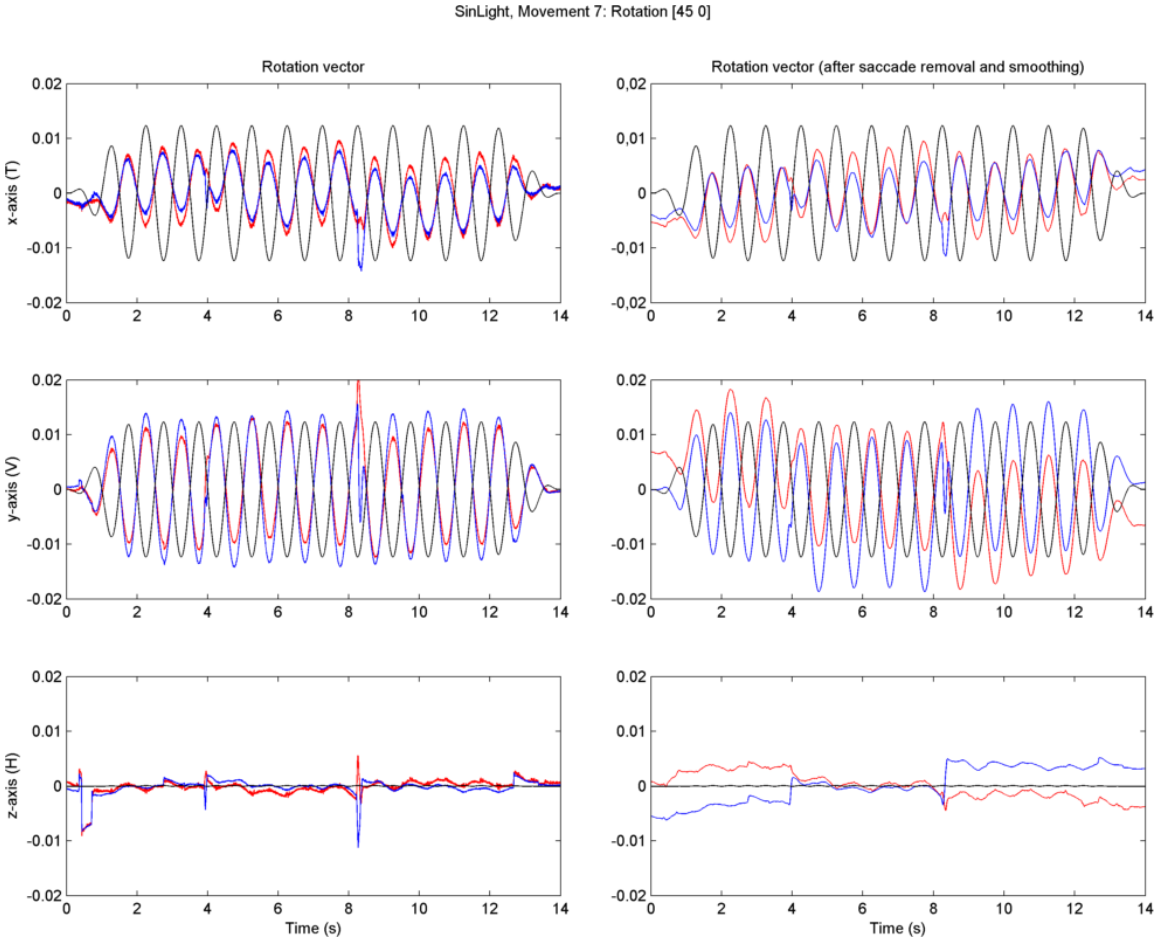

FIGURE 2.7: *Eye movements for sinusoidal stimulation in the light around an axis between roll and pitch (45° azimuth), thus mainly consisting of a torsion and vertical component. From top to bottom: x-axis (torsion), y-axis (vertical) and z-axis (horizontal) rotation. The stimulus and eye movements are denoted by the black and blue/red traces, respectively. The right panel shows the component rotation vectors after desaccading and smoothing.*

Platform position, which was defined by its azimuth, elevation and amplitude, was also transformed into Fick angles as rotation vectors, before being similarly converted to angular velocity. Component and 3-D eye velocity gains for sinusoidal stimulation were calculated by fitting a sinusoid with the platform frequency (1 Hz) through the horizontal, vertical and torsional angular velocity components(see Fig. 2.8). Fitting is done through all component traces, each having its own phase as a fit parameter.

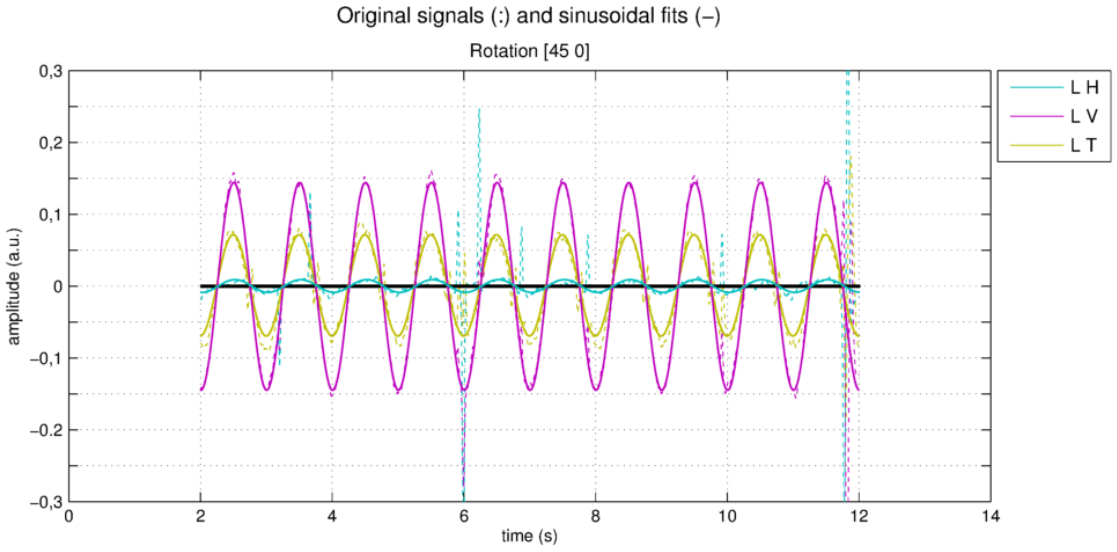

FIGURE 2.8: *Left eye angular velocity traces for sinusoidal stimulation in the light around an axis between roll and pitch (45° azimuth), thus mainly consisting of a torsion and vertical component. Shown here are the original component signals (dashed lines) and their corresponding sinusoidal fits (solid lines). Fade-in and fade-out time is excluded.*

Component gains were calculated either per left eye or each eye separately. Left and right eye data from binocular subjects was pooled. Misalignment of the coil in the eye was determined from fixation data of the target straight ahead ("0°") relative to the orthogonal primary magnetic field coils. Correction for this offset misalignment in the signals took place by 3-D counter rotation. The misalignment between the 3-D eye velocity and head velocity axes was obtained using the approach of Aw[20](see Appendix A). The misalignment is calculated as the instantaneous angle in 3-D between the head velocity (i.e. platform velocity) axis and the inverse of the eye velocity axis, using the scalar product of two vectors. The inverse of eye velocity ensures that the misalignment equals zero when head and eye velocity axis are perfectly aligned and opposite in direction. The misalignment only indicates that the eye rotation axis lies on a cone around the head rotation axis, which is why gaze plane plots are used to determine the deviation of the eye rotation in the yaw, roll and pitch planes (Figure 3.2).

All transients were individually observed. Traces of transients during which the subject blinked were manually discarded, which necessitated the omission of one subject for transients (such that $n = 5$ for transients). Only the first 100 ms after onset of the movement was considered, in which angular velocity components were averaged in time bins of 20 ms and plotted as a function of the platform velocity (see Fig. 2.9)[21][22]. The acceleration of the transients was constant during the first 100 ms, so that the slopes of the linear regression line fitted through the time bins are a direct measure for eye velocity gain. Left and right eye gains were averaged.

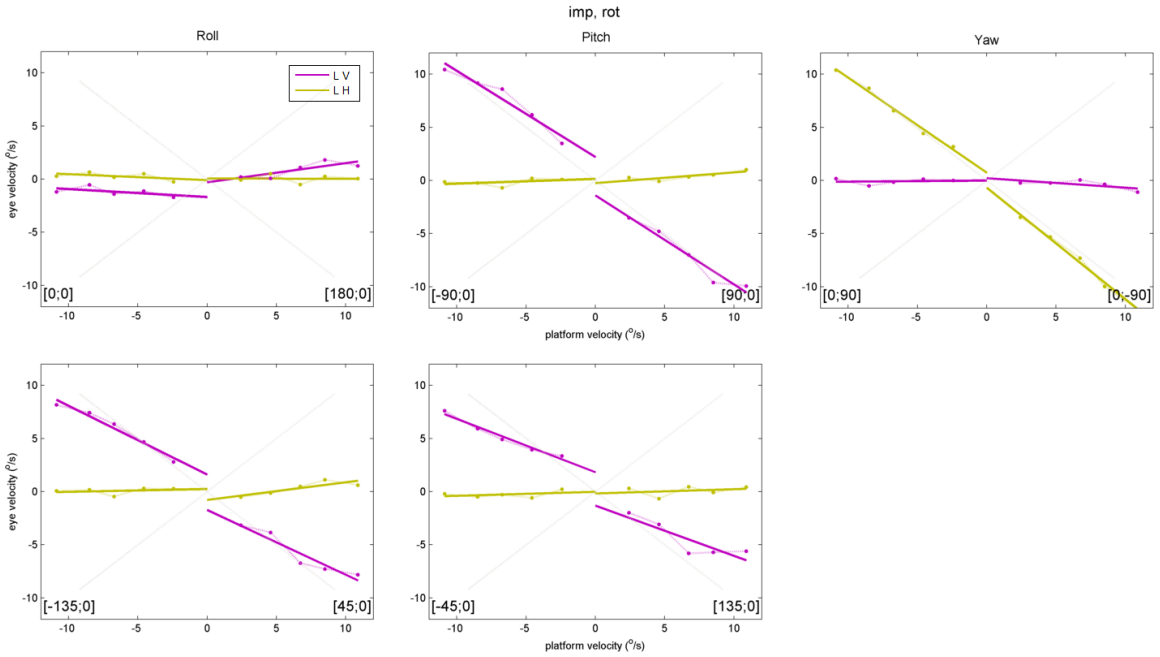

FIGURE 2.9: *Eye velocity - head velocity plots during angular transients in one subject. Only the vertical and horizontal components for the left eye are shown. Each filled circle is one bin (bin width=20 ms) of mean eye velocity of max. 3 repetitions of the impulse. Top row: impulses around the cardinal axes, bottom row: impulses around the axes between roll and pitch. Eye movements are shown for both CW and CCW rotation per rotation axis.*

2.7 Statistical Analysis

Repeated measures analysis of variance was used to test for significant differences between light conditions within all head positions for sinusoidal and transient stimulation. Wilcoxon's signed-rank test was used to test for significant differences between initial head positions for both types of stimuli. All analyses were done with a significance $p = 0.05$.

Chapter 3

Results

3.1 Sinusoidal Stimulation

3.1.1 *Head upright* (0°)

Sinusoidal yaw rotation (vertical axis) yielded smooth compensatory eye movements with occasional saccades. The mean gain ± one standard deviation (N=6) was 1.01 ± 0.04 in the light. The responses were made up of the horizontal eye movement component, while the vertical and torsional components were very small (< 0.04). In darkness (imagined target), saccades interrupted the compensatory eye movements more frequently, which was paired with a small drift of the other components in most subjects. 3-D vector gain during vertical axis rotation in darkness was 0.70 ± 0.18. The misalignment ± one standard deviation (N=6) was 3.10° ± 1.25° in the light, and 5.85° ± 3.53° in darkness.

For horizontal axis stimulation, each components relative contribution to the gain depended on the orientation of the stimulus axis. Torsion was the major component of the response when the stimulus axis was in the naso-occipital direction (roll), with a mean gain of 0.39 ± 0.06 in the light and 0.35 ± 0.06 in darkness (see Figure 3.1).

Stimulation about axes between interaural and naso-occipital yielded a combination of torsion and vertical components in the compensatory eye movements. For rotation around the interaural axis, the vertical component had near unity gain at 0.98 ± 0.09 in the light, and 0.86 ± 0.08 in darkness. Ocular drift during sinusoidal stimulation was observed to be more frequent in darkness than in the light. The standard deviations of the misalignment in light and in darkness respectively were 3.81° and 11.51° during roll stimulation, and 0.79° and 1.43° during pitch stimulation.

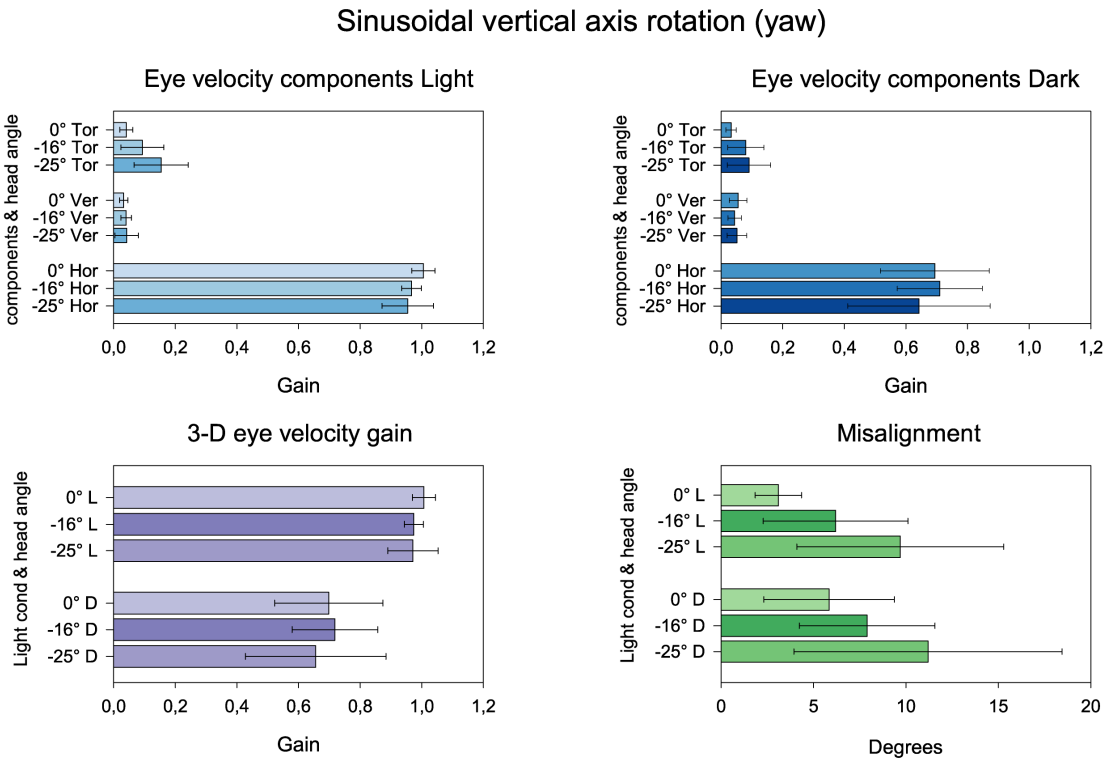

FIGURE 3.1: *Eye velocity component gains, 3-D velocity gain and misalignment results for sinusoidal yaw rotation averaged over all subjects (N=6) in the light, dark, and for the three head orientations.*

Eye movements were mainly confined to vertical and/or torsion eye velocities during horizontal axis stimulation. The dashed lines in Figures 3.2 and 3.3 show the mean gain of the horizontal, vertical and torsion components over the range of tested stimulation axes in the horizontal plane. Torsion was maximal during roll rotation (0°), while vertical peaked during pitch (90°). The contributions of vertical and torsion eye movements were inversely related between -45° and 45° azimuth. 3-D eye velocity gain varied between 0.98 ± 0.09 (pitch) and 0.40 ± 0.06 (roll) in the light, and 0.87 ± 0.08 and 0.38 ± 0.06 in darkness.
Misalignment in the light between stimulus (head rotation) and response (eye rotation) axis was smallest during pitch (3.20°) and gradually increased approaching the stimulus axis orientation at 22.5° azimuth (maximum misalignment 27.45°), to decrease again towards the roll axis (16.22°).
The maximum gains of vertical and torsion components were lower in darkness than in the light (torsion: 0.35 ± 0.06, vertical: 0.86 ± 0.08). 3-D eye velocity gain values were significantly lower than in the light (RANOVA, $p < 0.04$). Contrary to previous results [13], misalignment differences between light conditions were not as pronounced, with significant differences only present at pitch rotation (RANOVA, $p = 0.05$). The spread during darkness however was larger, having a maximal standard deviation of 11.51° compared

to 4.34° in the light. Horizontal gain was slightly higher in darkness than during light ($0.04 < gain < 0.1$), however not significantly so.

3.1.2 *Head pitched down* (16°)

Rotating the head nose-down by 16° aligned the horizontal canal's prime direction with the E-H. This initial head position yielded results close to those obtained with the head upright (see Figure 3.1), albeit significantly higher for the torsion component during sinusoidal yaw rotation, and significantly lower for the torsion and vertical components during stimulation about several axes between interaural and naso-occipital (see Figure3.2); these differences will be expanded upon below.

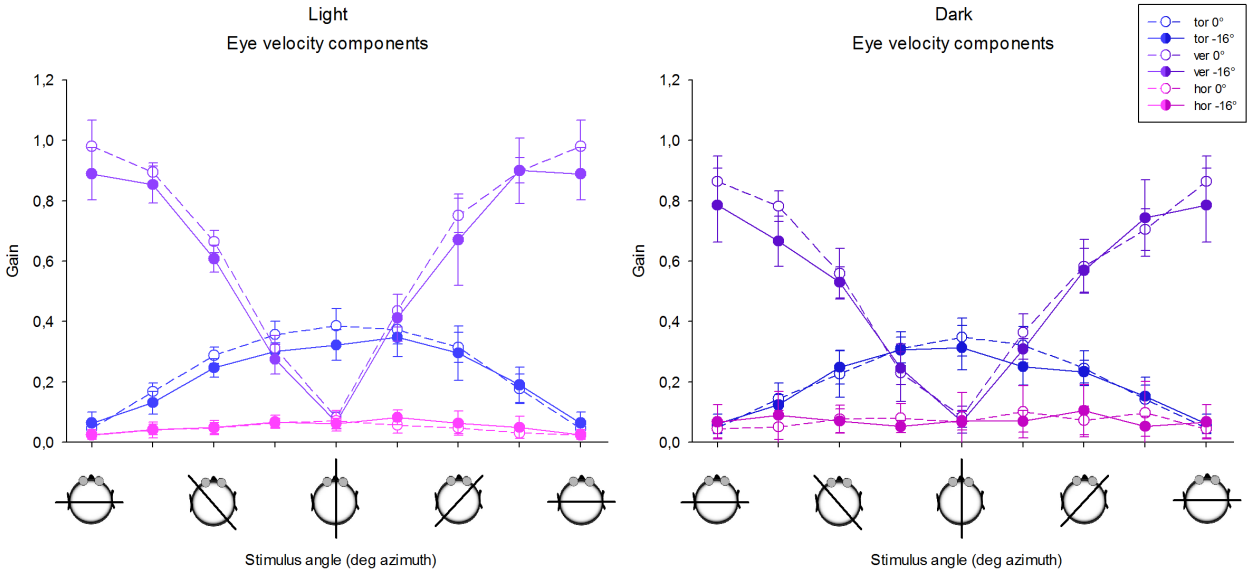

FIGURE 3.2: *Eye velocity component results for all tested horizontal stimulus axes averaged over all subjects (N=6) in the light (left), dark (right), and for the head upright (dashed) and pitched down 16° (solid).*

Yaw rotation yielded smooth compensatory eye movements with occasional saccades, with an increase in the torsion component in the light (0.08 ± 0.06) and a statistically significant increase in darkness compared with head upright at 0.09 ± 0.07 ($Z = -1.992$, $p = 0.046$). The contribution of the vertical and horizontal components in the light as well as in darkness remained unchanged compared to the head upright. 3-D velocity gain also did not change for both light conditions, while the misalignment in the light increased significantly with 3.10° ($Z = -2.201$, $p = 0.028$).

Significant differences between component gains during stimulation around axes between interaural appeared asymmetrical and exclusively lower (see Figure 3.2), while limited to

the torsion and vertical component. A comparison between the head positions and significant differences is shown in tables 3.1 and 3.2 for stimulation in the light and in darkness, respectively. While the horizontal component remained equivalent in both head positions and light conditions, the torsion and vertical components were subject to a decrease in mean gain around several rotation axes. This was more evident in the light than in darkness, especially for the vertical component. Interestingly, none of the rotation axes for which there was a significant gain decrease in the light appeared to significantly decrease in darkness. Contrary to the head upright, the torsion component's maximum mean gain is not during roll, but during 22.5° in the light, and -22.5° in darkness. No significant differences for the misalignment were observed during horizontal plane stimulation in the light, while in darkness it increased with 2.84° ($Z = -1.992$, $p = 0.046$) around 90° azimuth. 3-D velocity was significantly lower for this head position around rotation axes 90° and 45° azimuth in the light, and decreased around -67.5° and 22.5° azimuth during darkness (see Figure 3.4).

3.1.3 *Head pitched down* (25°)

Rotating the head nose-down by 25° aligned the horizontal canal's anatomical plane (and thus its maximal response direction) with the E-H. Sinusoidal stimulation with the head in this position yielded results very similar to stimulation with the head pitched down 16°. While a pattern is distinguishable in i.e. 3-D eye velocity gain and misalignment (decreasing velocity gain and increasing misalignment as nose-down pitch angle increases, see Figure 3.4), the statistically significant differences between 16° and 25° nose-down only occur around a few rotation axes (see appendix B). Mean component gains, SDs and significant p-values between the head upright and pitched down 25° can be found in tables 3.3 and 3.4. A decrease in component gain with respect to the head upright is apparent, and for this head position is also present for the horizontal component in darkness (see Figure 3.3, *right*).

Overall, component and 3-D velocity gain decrease while misaligments increase. As such, VOR quality seems to worsen as the downward pitch angle increases for sinusoidal stimulation in the horizontal plane. For vertical axis rotation, torsion component gain increases with greater downward pitch, while horizontal component gain slightly decreases. 3-D velocity gain remains steady throughout the different head pitch angles, while misalignment increases more dramatically with increasing downward pitch. VOR quality appears to deteriorate in a similar manner when the head is pitched upward. A trial with sinusoidal stimuli was also performed on two subjects who were oscillated with their head upright, and with their head pitched nose-up 18° (see Appendix C).

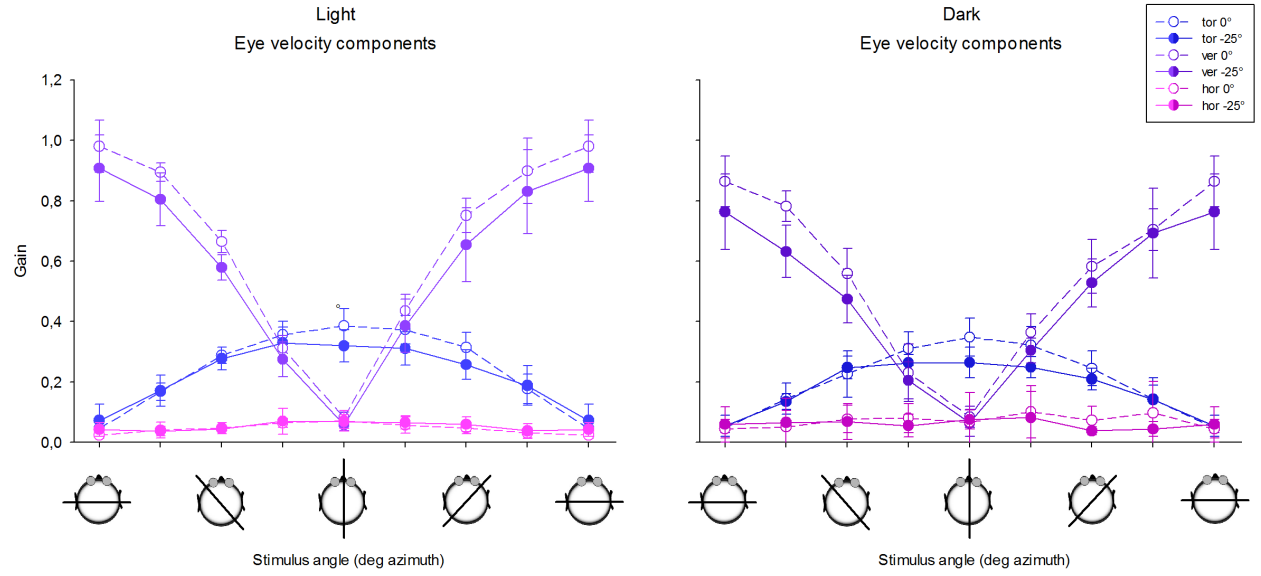

FIGURE 3.3: *Eye velocity component results for all tested horizontal stimulus axes averaged over all subjects (N=6) in the light (left), dark (right), and for the head upright (dashed) and pitched down 25° (solid).*

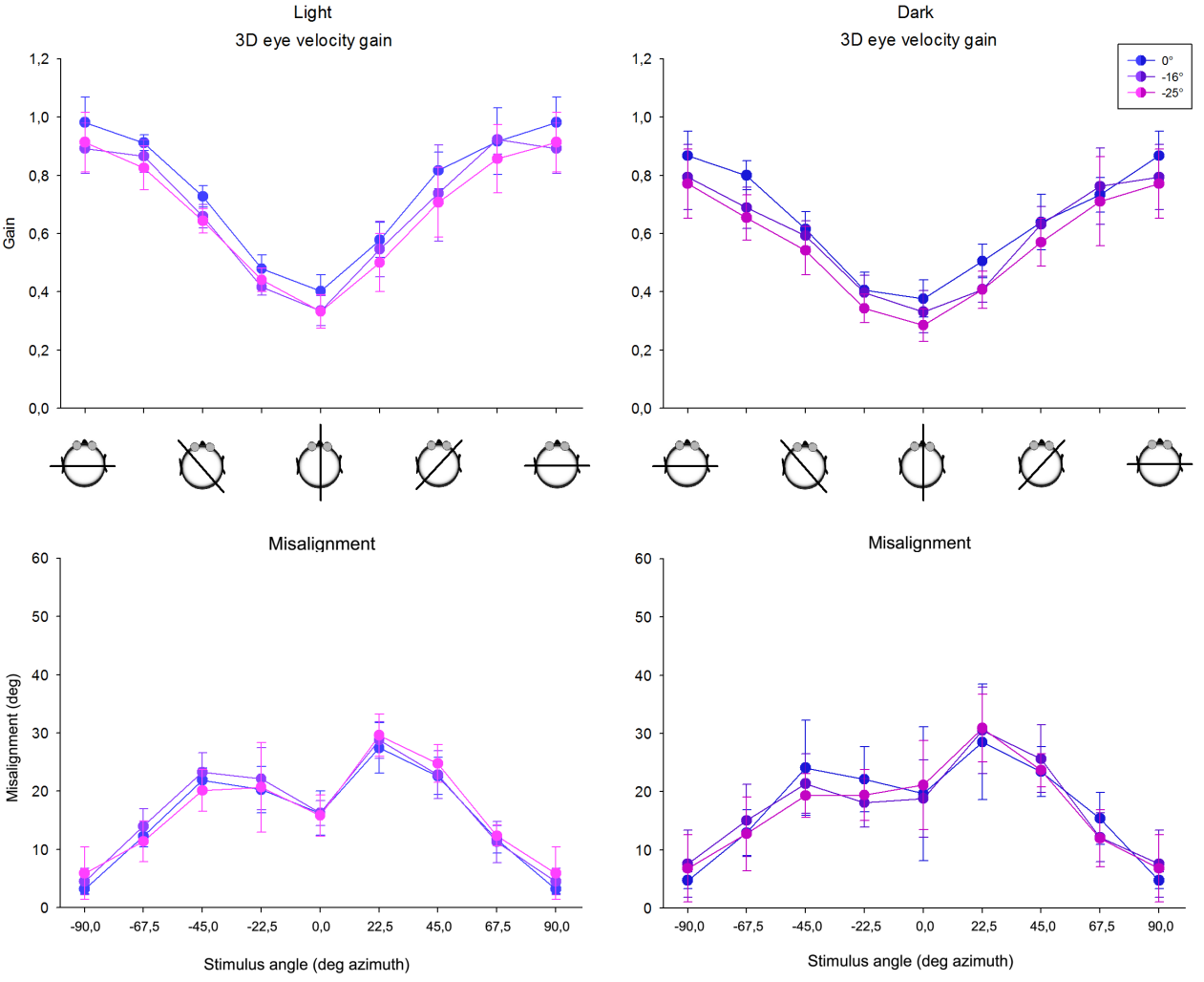

FIGURE 3.4: *Eye velocity component results for all tested horizontal stimulus axes averaged over all subjects (N=6) in the light, dark, and for the three head orientations.*

		Torsion			**Vertical**			**Horizontal**		
Rot. ax	*Angle*	*Mean*	*SD*	*p*	*Mean*	*SD*	*p*	*Mean*	*SD*	*p*
-90°	0°	0.05	0.02		0.98	0.09		0.02	0.01	
	−16°	0.06	0.04	-	0.89	0.09	0.028	0.03	0.02	-
−67.5°	0°	0.17	0.03		0.89	0.03		0.04	0.03	
	−16°	0.13	0.04	0.028	0.85	0.06	-	0.04	0.02	-
−45°	0°	0.29	0.03		0.67	0.04		0.05	0.02	
	−16°	0.25	0.03	0.028	0.61	0.04	0.028	0.05	0.02	-
−22.5°	0°	0.36	0.04		0.31	0.04		0.06	0.01	
	−16°	0.30	0.03	-	0.27	0.05	0.046	0.07	0.02	-
0°	0°	0.39	0.06		0.08	0.02		0.07	0.03	
	−16°	0.32	0.05	-	0.07	0.02	0.028	0.06	0.02	-
22.5°	0°	0.37	0.05		0.44	0.05		0.06	0.03	
	−16°	0.35	0.06	-	0.41	0.08	-	0.08	0.02	-
45°	0°	0.31	0.05		0.75	0.06		0.05	0.02	
	−16°	0.30	0.09	-	0.67	0.15	-	0.06	0.04	-
67.5°	0°	0.18	0.05		0.90	0.11		0.03	0.02	
	−16°	0.19	0.06	-	0.90	0.04	-	0.05	0.04	-
90°	0°	0.05	0.02		0.98	0.09		0.02	0.01	
	−16°	0.06	0.04	-	0.89	0.09	0.028	0.03	0.02	-

TABLE 3.1: ***Light:*** *Mean component gains and standard deviations during sinusoidal rotation around axes in the horizontal plane with the head upright (0°) versus pitched down 16°, averaged over all subjects (N=6). P-values are only shown for the significantly different rotation axes. Wilcoxon's signed rank test was used for statistical analysis.*

		Torsion			**Vertical**			**Horizontal**		
Rot. ax	*Angle*	*Mean*	*SD*	*p*	*Mean*	*SD*	*p*	*Mean*	*SD*	*p*
-90°	0°	0.05	0.02		0.86	0.08		0.04	0.03	
	−16°	0.06	0.03	-	0.79	0.12	-	0.07	0.06	-
−67.5°	0°	0.15	0.05		0.78	0.05		0.05	0.05	
	−16°	0.12	0.03	-	0.67	0.08	0.028	0.09	0.08	-
−45°	0°	0.23	0.08		0.56	0.08		0.08	0.05	
	−16°	0.25	0.06	-	0.53	0.05	-	0.07	0.04	-
−22.5°	0°	0.31	0.06		0.23	0.10		0.08	0.05	
	−16°	0.31	0.04	-	0.25	0.05	-	0.05	0.02	-
0°	0°	0.35	0.06		0.08	0.03		0.07	0.10	
	−16°	0.31	0.07	-	0.07	0.04	-	0.07	0.03	-
22.5°	0°	0.32	0.06		0.36	0.06		0.10	0.09	
	−16°	0.25	0.06	0.028	0.31	0.03	-	0.07	0.04	-
45°	0°	0.25	0.06		0.58	0.09		0.07	0.05	
	−16°	0.23	0.04	-	0.57	0.07	-	0.11	0.09	-
67.5°	0°	0.14	0.05		0.70	0.07		0.10	0.10	
	−16°	0.15	0.06	-	0.74	0.13	-	0.05	0.03	-
90°	0°	0.05	0.02		0.86	0.08		0.04	0.03	
	−16°	0.06	0.03	-	0.79	0.12	-	0.07	0.06	-

TABLE 3.2: ***Dark:*** *Mean component gains and standard deviations during sinusoidal rotation around axes in the horizontal plane with the head upright (0°) versus pitched down 16°. P-values are only shown for the significantly different rotation axes. Wilcoxon's signed rank test was used for statistical analysis.*

		Torsion			**Vertical**			**Horizontal**		
Rot. ax	*Angle*	*Mean*	*SD*	*p*	*Mean*	*SD*	*p*	*Mean*	*SD*	*p*
-90°	0°	0.05	0.02		0.98	0.09		0.02	0.01	
	−25°	0.07	0.05	-	0.91	0.11	0.028	0.04	0.02	-
−67.5°	0°	0.17	0.03		0.89	0.03		0.04	0.03	
	−25°	0.17	0.05	-	0.80	0.09	0.028	0.04	0.02	-
−45°	0°	0.29	0.03		0.67	0.04		0.05	0.02	
	−25°	0.28	0.04	-	0.58	0.04	0.028	0.04	0.01	-
−22.5°	0°	0.36	0.04		0.31	0.04		0.06	0.01	
	−25°	0.33	0.05	-	0.28	0.06	-	0.07	0.04	-
0°	0°	0.39	0.06		0.08	0.02		0.07	0.03	
	−25°	0.32	0.05	-	0.06	0.02	0.028	0.07	0.02	-
22.5°	0°	0.37	0.05		0.44	0.05		0.06	0.03	
	−25°	0.31	0.06	0.028	0.39	0.09	0.046	0.07	0.02	-
45°	0°	0.31	0.05		0.75	0.06		0.05	0.02	
	−25°	0.26	0.05	0.028	0.65	0.12	0.028	0.06	0.02	-
67.5°	0°	0.18	0.05		0.90	0.11		0.03	0.02	
	−25°	0.19	0.06	-	0.83	0.14	-	0.04	0.02	-
90°	0°	0.05	0.02		0.98	0.09		0.02	0.01	
	−25°	0.07	0.05	-	0.91	0.11	0.028	0.04	0.02	-

TABLE 3.3: ***Light:*** *Mean component gains and standard deviations during sinusoidal rotation around axes in the horizontal plane with the head upright (0°) versus pitched down 25°. P-values are only shown for the significantly different rotation axes. Wilcoxon's signed rank test was used for statistical analysis.*

		Torsion			**Vertical**			**Horizontal**		
Rot. ax	*Angle*	*Mean*	*SD*	*p*	*Mean*	*SD*	*p*	*Mean*	*SD*	*p*
-90°	0°	0.05	0.02		0.86	0.08		0.04	0.03	
	−25°	0.06	0.04	-	0.76	0.13	-	0.06	0.06	-
−67.5°	0°	0.15	0.05		0.78	0.05		0.05	0.05	
	−25°	0.14	0.03	-	0.63	0.09	0.028	0.07	0.08	-
−45°	0°	0.23	0.08		0.56	0.08		0.08	0.05	
	−25°	0.25	0.04	-	0.47	0.08	0.028	0.07	0.06	-
−22.5°	0°	0.31	0.06		0.23	0.10		0.08	0.05	
	−25°	0.26	0.03	0.046	0.20	0.06	-	0.06	0.04	-
0°	0°	0.35	0.06		0.08	0.03		0.07	0.10	
	−25°	0.26	0.05	0.046	0.06	0.04	-	0.08	0.03	-
22.5°	0°	0.32	0.06		0.36	0.06		0.10	0.09	
	−25°	0.25	0.03	0.028	0.30	0.04	-	0.08	0.09	-
45°	0°	0.25	0.06		0.58	0.09		0.07	0.05	
	−25°	0.21	0.04	-	0.53	0.08	0.028	0.04	0.01	-
67.5°	0°	0.14	0.05		0.70	0.07		0.10	0.10	
	−25°	0.14	0.07	-	0.69	0.15	-	0.04	0.03	-
90°	0°	0.05	0.02		0.86	0.08		0.04	0.03	
	−25°	0.06	0.04	-	0.76	0.13	-	0.06	0.06	-

TABLE 3.4: ***Dark:*** *Mean component gains and standard deviations during sinusoidal rotation around axes in the horizontal plane with the head upright (0°) versus pitched down 25°. P-values are only shown for the significantly different rotation axes. Wilcoxon's signed rank test was used for statistical analysis.*

3.2 Transient Stimulation

For transient stimulation, only the horizontal and vertical components were included in the analysis due to deviant torsion (and thus 3-D vector gain and misalignment) data. Refer to Appendix D for more information.

3.2.1 *Head upright* (0°)

Yaw head transients yielded horizontal compensatory eye movements (see Figure 3.5). Horizontal component gain around the vertical axis was 0.91 for clockwise and 0.88 for counterclockwise head transients. For the head upright, there were no significant differences for the vertical and horizontal component mean values between left and rightward rotation. Contrary to what has been previously been reported, whole body transients around the interaural axis (pitch) resulted in nearly the same gains for pitch up and down for the horizontal and vertical components. Vertical component gain was 0.93 for upward pitch, and 0.97 for downward pitch, while being minimal during roll at 0.16 for clockwise rotation, and 0.12 for counterclockwise rotation. Horizontal component gain remained minimal over all rotation axes in the horizontal plane, with a minimum gain of 0.04 for counterclockwise rotation around -45° azimuth.

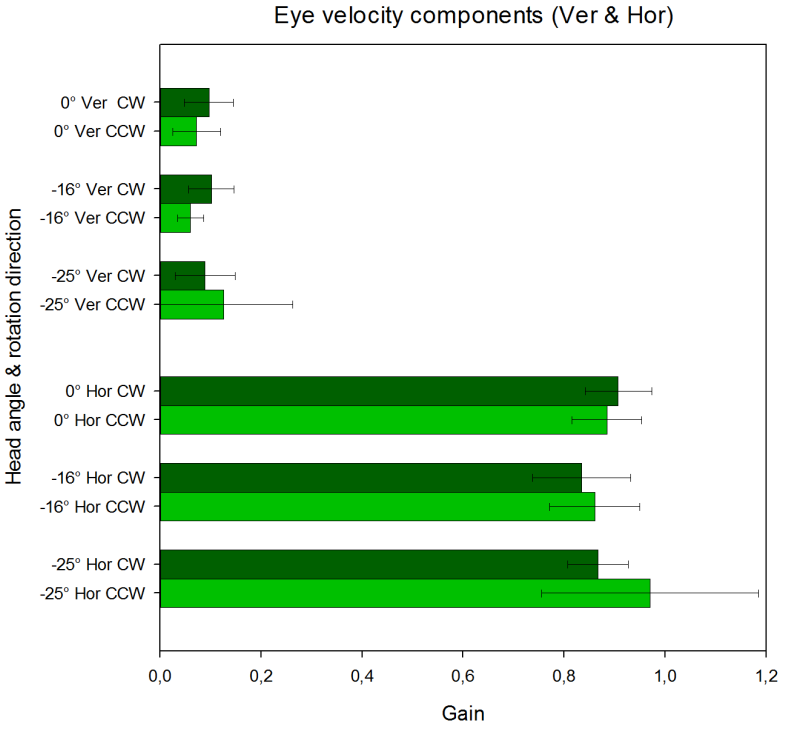

FIGURE 3.5: *Horizontal and vertical eye velocity component results for yaw transients in both rotation directions averaged over all subjects (N=5) for the three head orientations.*

3.2.2 *Head pitched down* (16°)

Yaw transients with the head pitched down 16° resulted in horizontal compensatory eye movements which were slightly lower than with the head upright, however not statistically significantly so, nor were the differences between CW and CCW rotation.
For rotations in the horizontal plane however, horizontal component gain appears notably higher than with the head upright around axes other than pitch and -45° azimuth for CW rotation, and 45° azimuth for CCW rotation. For some rotation axes, this difference between head upright and pitched down 16° is significant (see Table 3.5). This pattern also appears to be mirrored between CW and CCW rotation (see Figure 3.6).
The vertical component appears slight lower that for the head upright, excluding the significant peak at -45° azimuth for CW rotation, which is not observed for CCW rotation. Vertical component gain is 0.80± 0.14 at this point, contrasted with a gain of 0.66± 0.05 for the head upright.

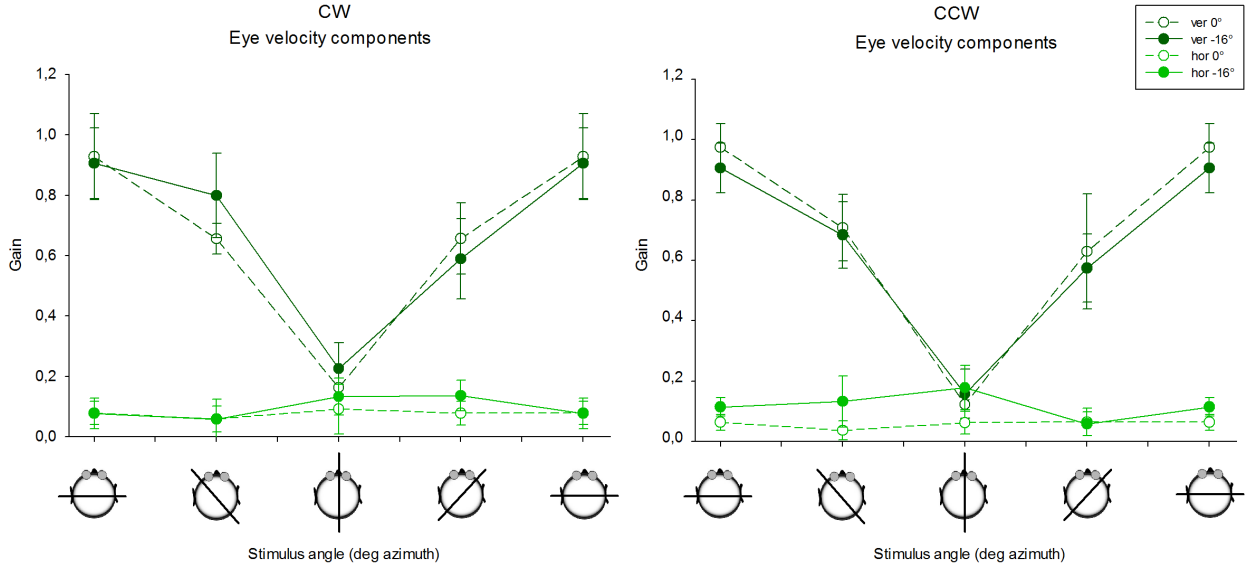

FIGURE 3.6: *Eye velocity component results for all tested horizontal stimulus axes averaged over all subjects (N=5) in the light (left), dark (right), and for the head upright (dashed) and pitched down 16° (solid).*

3.2.3 *Head pitched down* (25°)

Yaw transients with the head pitched down 25° were also not notably different from the other head orientations, though there does appear to be an increase in horizontal component gain compared to the head pitched down 16° for CW rotation. Mean horizontal gain for CCW is notably higher than for the other head orientations, but this is offset by its large standard deviation (0.97± 0.21).
Transient stimulation around axes in the horizontal plane in this head position resulted in

gains strongly deviating from the head upright gains. Like with the head pitched down 16°, horizontal component gain is higher for all rotation axes excluding interaural (pitch) for both rotation directions (see Figure 3.7). Vertical component gains appear especially erratic: around roll, the gains are higher than for the head upright for both rotation directions, while much lower for CW pitch rotation. Transients around 45° azimuth yield a much lower gain compared to the head upright for both rotation directions. Neither the horizontal nor the vertical component gains appear symmetrical between CW and CCW rotation.

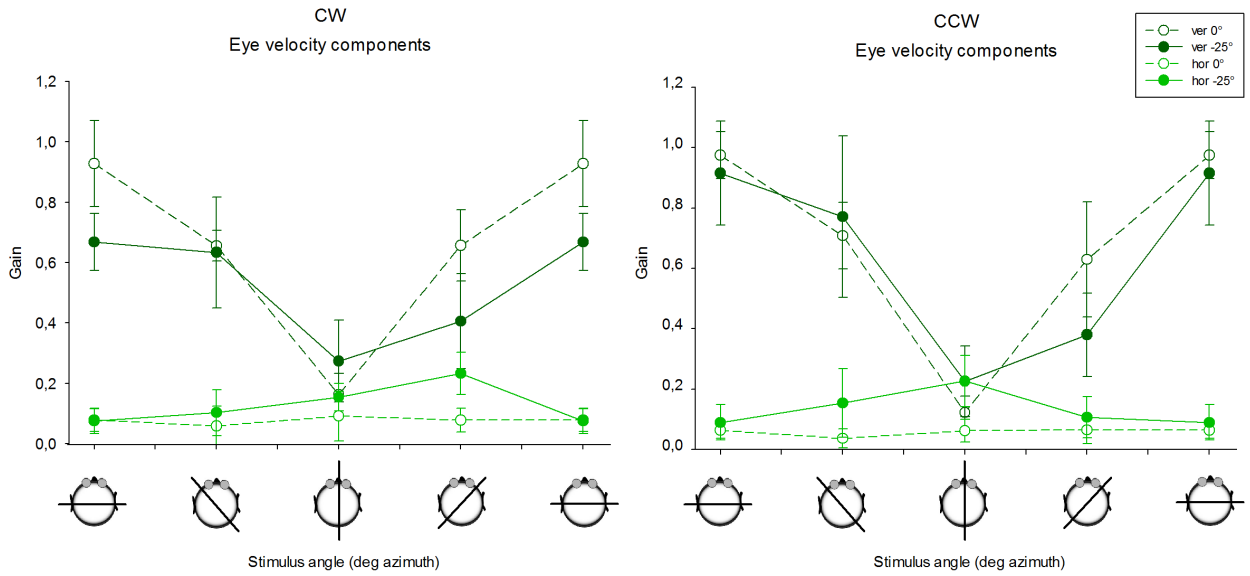

FIGURE 3.7: *Eye velocity component results for all tested horizontal stimulus axes averaged over all subjects (N=5) in the light (left), dark (right), and for the head upright (dashed) and pitched down 25° (solid).*

Overall, horizontal and vertical component gains for head upright transient stimulation are similar to those found for sinusoidal stimulation in the dark. For the pitched down head positions, the horizontal component gain has higher presence and more variety in its course during transient stimulation than during sinusoidal stimulation. Vertical component gain during transient stimulation is also markedly different from sinusoidal stimulation for nose down pitch, showing a much greater decrease and irregularity among the rotation axes.

		Vertical CW			**Horizontal CW**			**Vertical CCW**			**Horizontal CCW**		
Rot. ax	*Angle*	*Mean*	*SD*	*p*	*Mean*	*SD*	*p*	*Mean*	*SD*	*p*	*Mean*	*SD*	*p*
-90°	0°	0.93	0.14		0.08	0.04		0.97	0.08		0.06	0.03	
	−16°	0.91	0.12	-	0.08	0.05	-	0.91	0.08	-	0.11	0.03	-
−45°	0°	0.66	0.05		0.06	0.07		0.71	0.11		0.04	0.03	
	−16°	0.80	0.14	-	0.06	0.04	-	0.68	0.11	-	0.13	0.09	-
0°	0°	0.16	0.07		0.09	0.08		0.12	0.05		0.06	0.04	
	−16°	0.23	0.09	-	0.13	0.06	-	0.16	0.08	0.043	0.18	0.07	0.043
45°	0°	0.66	0.12		0.08	0.04		0.63	0.19		0.07	0.05	
	−16°	0.59	0.13	0.043	0.14	0.05	-	0.57	0.11	0.043	0.06	0.04	-
90°	0°	0.93	0.14		0.08	0.04		0.97	0.08		0.06	0.03	
	−16°	0.91	0.12	-	0.08	0.05	-	0.91	0.08	-	0.11	0.03	-

TABLE 3.5: *Mean component gains and standard deviations during transients around axes in both directions in the horizontal plane with the head upright (0°) versus pitched down 16°. P-values are only shown for the significantly different rotation axes. Wilcoxon's signed rank test was used for statistical analysis.*

		Vertical CW			**Horizontal CW**			**Vertical CCW**			**Horizontal CCW**		
Rot. ax	*Angle*	*Mean*	*SD*	*p*	*Mean*	*SD*	*p*	*Mean*	*SD*	*p*	*Mean*	*SD*	*p*
-90°	0°	0.93	0.14		0.08	0.04		0.97	0.08		0.06	0.03	
	−25°	0.56	0.36	-	0.08	0.04	-	0.92	0.17	-	0.09	0.06	-
−45°	0°	0.66	0.05		0.06	0.07		0.71	0.11		0.04	0.03	
	−25°	0.47	0.31	-	0.10	0.08	-	0.77	0.27	-	0.15	0.11	-
0°	0°	0.16	0.07		0.09	0.08		0.12	0.05		0.06	0.04	
	−25°	0.14	0.06	-	0.15	0.04	0.043	0.23	0.12	-	0.23	0.08	-
45°	0°	0.66	0.12		0.08	0.04		0.63	0.19		0.07	0.05	
	−25°	0.42	0.24	-	0.23	0.07	-	0.38	0.14	0.043	0.11	0.07	0.043
90°	0°	0.93	0.14		0.08	0.04		0.97	0.08		0.06	0.03	
	−25°	0.56	0.36	-	0.08	0.04	0.043	0.92	0.17	0.043	0.09	0.06	-

TABLE 3.6: *Mean component gains and standard deviations during transients around axes in both directions in the horizontal plane with the head upright (0°) versus pitched down 25°.*

Chapter 4

Discussion and Conclusions

The aim of this study was to quantify the relative dependency of the 3-D VOR on canal anatomy and orientation. More specifically, we singled out the horizontal canals due to their distinct upward inclination with respect to the E-H. In this study we show that in practice, stimulation around the mathematically modeled maximum response directions and prime directions do not precisely produce the expected results for the horizontal canals, for both sinusoidal and transient stimulation. Stimulation with the head upright yields superior gains and lowest misalignments despite the horizontal canal planes deviation from the E-H, with the exception of the horizontal component during transient stimulation. This suggests that the VOR is optimized for the head in an upright position, leading to the assumption that other mechanisms override the influence of the distinct horizontal canal orientation.
For sinusoidal stimulation around axes in the horizontal plane (roll, pitch and axes in between), a decrease in gain for the torsion and vertical components and higher misalignment was found for increasing downward pitch, while horizontal component gain remained minimal. A decrease in torsion gain is geometrically appropriate as it is expected to fall with eccentric gaze in any direction[23]. This was observed both in the light and darkness. For sinusoidal vertical axis rotation (yaw), increasing downward pitch resulted in increasing misalignment, decreasing horizontal gain, unchanged minimal vertical component gain and an increase in torsion component gain. This increase in torsion was also observed in upward pitch and is imparted by the lateral and medial recti [24]. This adherence to the cosine rule was not found in the horizontal component, the decrease of which for yaw and lack of change during roll rotation contradicts the notion that aligning the horizontal anatomical canal plane closer to the E-H improves the horizontal 3-D VOR. While the composition of components was to some degree expected to vary for different head pitch angles due to attenuation of gains by the cosine of the angle between the optical axis and plane of head rotation, 3-D velocity gains decreased slightly but distinctly for increasing downward and upward head pitch for both light conditions, indicating that head upright yields the highest

quality 3-D VOR.
Yaw head transients delivered with the head in different initial positions resulted in overall similar data, both between head positions and between rotation directions. Contrary to previously reported[13], pitch up and pitch down transients with the head upright resulted in nearly the same horizontal and vertical component gains. The most notable finding for transient stimulation around axes in the horizontal plane, was that the horizontal component gain was minimal for the head upright, but increased for both rotation directions as the initial head position was pitched further downwards. This increase was not seen in our control subjects that had their head pitched upwards; in that case the horizontal component gain was not significantly different than for the head upright. The vertical component gain for the head pitched down 16°, was higher around several horizontal plane rotation axes, and lower in others. The difference in gain becomes dramatic with the head pitched down 25°, wherein, for both rotation directions, the vertical component gain is higher than upright for roll, and lower than upright for pitch. This effect was more strongly present for clockwise rotation. The symmetrical deviation of the component gains for the head tilted down 16° with respect to upright, was also lost when the head was pitched down 25°.

Sinusoidal and transient stimulation was delivered to the subject while they focused on a target (red LED) which was in the line of sight when the subject was seated upright looking straight ahead. Pitching the head down and up during the experiments led to different sagittal eye-in-orbit positions for each head pitch position. The decrease in VOR quality at head pitch positions other than upright is however not attributable to eye position signals, as they - whether efference-copy related or proprioceptive - do not interfere with normal human VOR [25], when the rotation directions (in this case: planes of action of the extraocular muscles) are independent of eye position [24].

3-D VOR during sinusoidal whole-body rotations for the head pitched down and up appears to be of lesser quality than for the head upright as pitch angle increases. Increase of horizontal component gain did not occur, while yaw rotations for pitched head positions contained a larger torsion component. Transients yielded similar results, with the most important difference being the increase of horizontal component gain with increasing downward head pitch angle during rotation around axes in the horizontal plane. Curiously, this increase in the horizontal component gain was not observed for yaw stimulation.

The obtained results do not provide supportive evidence for complete anatomical dependence of the 3-D VOR, and while they point more towards the head upright being the ideal head position, the data is still incongruent and even contradictory on some counts. This raises the question of whether other mechanisms are of influence on the 3-D VOR during whole-body stimulation, and if and how the effects of these mechanisms are influenced by different head pitch positions. Changing the head pitch position influences the semicircular

canal orientation with gravity, which possibly has an effect on the canals' response vectors. Tilting the head yields an effect from the otolith organs, which possibly influences central integration between canal and otolith signals[13]. Besides yaw rotation with the head upright, all oscillations around all different rotation axes were gravity-assisted as the gravity vector is continuously perceived by the otoliths. As such they were stimulated, both dynamically due to horizontal axis rotation, due to the different initial pitch head positions, tilting the otoliths[26]. According to Einstein's equivalence principle, tilt and translation induce physically equivalent inertial accelerations of the otoconia[27]. It has however, been established that the linear VOR (LVOR) response to head tilt works primarily at low frequencies, while LVOR responses to head translation act at higher frequencies[28]. As we oscillated subjects sinusoidally at a relatively low frequency (1 Hz), and translational LVOR sensitivity becomes significant for near targets while ours was distant[28], mainly the LVOR response to head tilt is considered relevant here. For rotations near roll, target eccentricity also heightens LVOR sensitivity, which possibly had a role in the increase of horizontal as well as vertical component gain for increased pitch during roll for transient stimulation. Also, during transients, higher accelerations are attained such that non-linear VOR pathways may be recruited, leading to higher gains, in this case mostly found for the horizontal component[26].

Besides its constant presence under Earth-bound conditions, recent findings have demonstrated that the gravity vector represents a common reference for vestibular and oculomotor responses[29]. Under prolonged microgravity during spaceflight (effective absence of gravity), the reference coordinate frame of the 3-D VOR is consistently tilted forward. This is indicative of the gravity-induced, otolith-mediated VOR component present during roll rotation under Earth-bound conditions. Listing's plane (the plane orthogonal to the primary position[30]) however, tilts backwards under microgravity, and may point towards a dis-inhibition in the control of torsional eye position. This implies that the otolith-mediated gravity vector has an inhibitory effect on torsional eye position[29]. This might explain the reduction in 3-D VOR gain during sinusoidal rotations around axes in the horizontal plane (most notably the torsion component around roll as seen in 3.2, 3.3 and C.2) while the head is pitched up or down, tilting the otoliths. However, the same effect is seen during the dark condition for sinusoidal stimulation, while Listing's law is only applicable to visual directions of sight[31]. It is possible however that the LED presented during the stationary period in between movements combined with memory and prediction still have an influence. This inhibition of the components around roll is not observed during transient stimulation, which can be attributed to the otoliths' low-pass behaviour, as the gravity effect decreases with frequency[32].

4.1 Study limitations

Several subjects reported discomfort and/or fatigue while in the lowest pitch position, as they had to strain turning their eyes upwards to look at the target. The stationary target could therefore still be considered a limitation of this study. It could prove to be useful to repeat the experiment with a variable target that keeps the subjects line of sight in the plane of horizontal head rotation for all head pitch angles. Another shortcoming is the small number of subjects. While their responses for sinusoidal stimulation are consistent and distinctly different between head positions, these findings would best be demonstrated in a larger group. A need to more clearly communicate the protocol to each subject became apparent, as several exclusions had to be made based on voluntary erroneous eye movements made by some subjects. It also became apparent that attention span, concentration and fatigue vary per subject and might be of influence on the data. A foolproof way of reducing the necessity of discarding unusable data, would be to conduct several clinical tests beforehand to determine whether or not the subject has ailments that could influence the data (i.e. sub-par vision, strabismus). A more robust way of positioning subjects of variable upper body length at the same height within the magnetic field is desirable, as is a more accurate method of varying head pitch angle (prevention of headband and biteboard movements, etc.).
As the emphasis of this study was placed on semicircular canal rotation and experimentation time per subject was limited, translational stimulation was excluded from the protocol. The results however raise an interest into the contribution of the otoliths, for which translational stimulation could provide more insight. Finally and most importantly, transient data was incomplete through the lack of torsion component data. This rendered our 3-D vector gain and misalignment data unusable, while these results could be especially insightful.

4.2 Future directions

It is evident that rotation around the naso-occipital axis is most insightful with respect to the role of the otoliths during head rotations. A more roll-centered approach could be taken in future studies, taking into account target eccentricity as well as multiple smaller variations of pitch and perhaps yaw angles. Considering the canals' and otoliths' different behaviour for various stimulation frequencies, it could be of interest to adjust the protocol such that a number of sinusoidal frequencies is tested. The sinusoidal frequency used here (1 Hz), is well within the operating range of the semicircular canals[33], but the functional range of the otoliths is narrower and around lower frequencies.

Appendix A

Misalignment Calculation

The misalignment angle is defined as the deviation of the eye rotation axis from perfect alignment with the head rotation axis in three dimensions, and is expressed as δ. Misalignment equals zero when there is perfect alignment, and when the eye velocity is opposite in direction to the head velocity. The head-fixed coordinate system is used as a common reference system, such that the direction of the head velocity needs to be transformed to space fixed coordinates $\vec{\omega}_h^{space}$. In this manner, head velocity can be referenced to the same head-fixed coordinates as eye velocity [34].

The misalignment is calculated as the instantaneous angle in 3-D between the head velocity axis and the inverse of the eye velocity acis, where the scalar product of these two vectors is used. δ measures the smaller angle between the two vectors when their initial points coincide. Using the inverse of eye velocity provides that misalignment is zero when there is perfect alignment between the head and eye velocity axes, and that eye velocity is in a direction opposite to head velocity. Head velocity as related to head-fixed coordinates is described by:

$$\delta = cos^{-1}\left(\frac{\vec{\omega}_e^{head} \cdot \vec{\omega}_h^{head}}{|\vec{\omega}_e^{head}| \cdot |\vec{\omega}_h^{head}|}\right) \tag{A.1}$$

Head velocity referenced to head-fixed coordinates $\vec{\omega}_h^{head}$and the rotation vector denoting current head position referenced to space-fixed coordinates $\vec{r}_h$ are given by

$$\vec{\omega}_h^{head} = \left(\vec{\omega}_h^{space} \cdot \vec{n}_h\right) * \vec{n}_h + \left(\vec{n}_h \times \vec{\omega}_h^{space}\right) * \sin\beta - \left[\vec{n}_h \times \left(\vec{n}_h \times \vec{\omega}_h^{space}\right)\right] * \cos\beta \tag{A.2}$$

$\vec{n}_h$ is a unit vector parallel to $\vec{r}_h$:

$$\vec{n}_h = \frac{\vec{r}_h}{|\vec{r}_h|} \tag{A.3}$$

The inverse of the rotation angle from the reference position to the current head position is given by

$$\beta = -2 * \tan^{-1}\left(|\vec{r}_h|\right). \tag{A.4}$$

Appendix B

Head pitched down 16° vs 25°

B.1 Sinusoidal Stimulation

		Torsion			**Vertical**			**Horizontal**		
Rot. ax	*Angle*	*Mean*	*SD*	*p*	*Mean*	*SD*	*p*	*Mean*	*SD*	*p*
-90°	−16°	0.06	0.04		0.89	0.09		0.03	0.02	
	−25°	0.07	0.05	-	0.91	0.11	-	0.04	0.02	-
−67.5°	−16°	0.13	0.04		0.85	0.06		0.04	0.02	
	−25°	0.17	0.05	-	0.80	0.09	-	0.04	0.02	-
−45°	−16°	0.25	0.03		0.61	0.04		0.05	0.02	
	−25°	0.28	0.04	-	0.58	0.04	-	0.04	0.01	-
−22.5°	−16°	0.30	0.03		0.27	0.05		0.07	0.02	
	−25°	0.33	0.05	-	0.28	0.06	-	0.07	0.04	-
0°	−16°	0.32	0.05		0.07	0.02		0.06	0.02	
	−25°	0.32	0.05	-	0.06	0.02	-	0.07	0.02	-
22.5°	−16°	0.35	0.06		0.41	0.08		0.08	0.02	
	−25°	0.31	0.06	0.046	0.39	0.09	-	0.07	0.02	-
45°	−16°	0.30	0.09		0.67	0.15		0.06	0.04	
	−25°	0.26	0.05	-	0.65	0.12	-	0.06	0.02	-
67.5°	−16°	0.19	0.06		0.90	0.04		0.05	0.04	
	−25°	0.19	0.06	-	0.83	0.14	-	0.04	0.02	-
90°	−16°	0.06	0.04		0.89	0.09		0.03	0.02	
	−25°	0.07	0.05	-	0.91	0.11	-	0.04	0.02	-

TABLE B.1: ***Light:*** *Mean component gains and standard deviations during sinusoidal rotation around axes in the horizontal plane with the head pitched down 16° versus 25°. P-values are only shown for the significantly different rotation axes. Wilcoxon's signed rank test was used for statistical analysis.*

		Torsion			**Vertical**			**Horizontal**		
Rot. ax	*Angle*	*Mean*	*SD*	*p*	*Mean*	*SD*	*p*	*Mean*	*SD*	*p*
-90°	−16°	0.06	0.03		0.79	0.12		0.07	0.06	
	−25°	0.06	0.04	0.042	0.76	0.13	-	0.06	0.06	-
−67.5°	−16°	0.12	0.03		0.67	0.08		0.09	0.08	
	−25°	0.14	0.03	-	0.63	0.09	-	0.07	0.08	-
−45°	−16°	0.25	0.06		0.53	0.05		0.07	0.04	
	−25°	0.25	0.04	-	0.47	0.08	-	0.07	0.06	-
−22.5°	−16°	0.31	0.04		0.25	0.05		0.05	0.02	
	−25°	0.26	0.03	-	0.20	0.06	-	0.06	0.04	-
−16°	0°	0.31	0.07		0.07	0.04		0.07	0.03	
	−25°	0.26	0.05	-	0.06	0.04	-	0.08	0.03	-
22.5°	−16°	0.25	0.06		0.31	0.03		0.07	0.04	
	−25°	0.25	0.03	-	0.30	0.04	-	0.08	0.09	-
45°	−16°	0.23	0.04		0.57	0.07		0.11	0.09	
	−25°	0.21	0.04	-	0.53	0.08	-	0.04	0.01	-
67.5°	−16°	0.15	0.06		0.74	0.13		0.05	0.03	
	−25°	0.14	0.07	-	0.69	0.15	-	0.04	0.03	-
90°	−16°	0.06	0.03		0.79	0.12		0.07	0.06	
	−25°	0.06	0.04	0.042	0.76	0.13	-	0.06	0.06	-

TABLE B.2: ***Dark:*** *Mean component gains and standard deviations during sinusoidal rotation around axes in the horizontal plane with the head pitched down 16° versus 25°. P-values are only shown for the significantly different rotation axes. Wilcoxon's signed rank test was used for statistical analysis.*

B.2 Transient Stimulation

		Vertical CW			**Horizontal CW**			**Vertical CCW**			**Horizontal CCW**		
Rot. ax	*Angle*	*Mean*	*SD*	*p*	*Mean*	*SD*	*p*	*Mean*	*SD*	*p*	*Mean*	*SD*	*p*
-90°	−16°	0.91	0.12		0.08	0.05		0.91	0.08		0.11	0.03	
	−25°	0.56	0.36	-	0.08	0.04	-	0.92	0.17	-	0.09	0.06	-
−45°	−16°	0.80	0.14		0.06	0.04		0.68	0.11		0.13	0.09	
	−25°	0.47	0.31	-	0.10	0.08	-	0.77	0.27	-	0.15	0.11	-
0°	−16°	0.23	0.09		0.13	0.06		0.16	0.08		0.18	0.07	
	−25°	0.14	0.06	-	0.15	0.04	-	0.23	0.12	0.043	0.23	0.08	-
45°	−16°	0.59	0.13		0.14	0.05		0.57	0.11		0.06	0.04	
	−25°	0.42	0.24	0.043	0.23	0.07	0.043	0.38	0.14	0.043	0.11	0.07	-
90°	−16°	0.91	0.12		0.08	0.05		0.91	0.08		0.11	0.03	
	−25°	0.56	0.36	0.043	0.08	0.04	-	0.92	0.17	-	0.09	0.06	-

TABLE B.3: *Mean component gains and standard deviations during transients around axes in both directions in the horizontal plane with the head pitched down 16° versus 25°.*

Appendix C

Control: Nose-up Pitch

C.1 Sinusoidal Stimulation

The effect of the head pitched upwards by 18° compared to the head upright was measured in three subjects for sinusoidal stimulation. Presumably due to the size of this control group, no statistically significant differences were found between the two head angles for sinusoidal stimulation. However, it is apparent from the means and the resulting figures that there is an effect resulting from pitching the head up: a consistent decrease in gain for the vertical and torsion component during stimulation around axes in the horizontal plane in the light as well as in darkness, causing an increase in misalignment. For yaw stimulation, gain most notably decreases for the horizontal component. During yaw stimulation in the light, torsion gain increases, similar to the torsion increase for the head pitched down measurements.

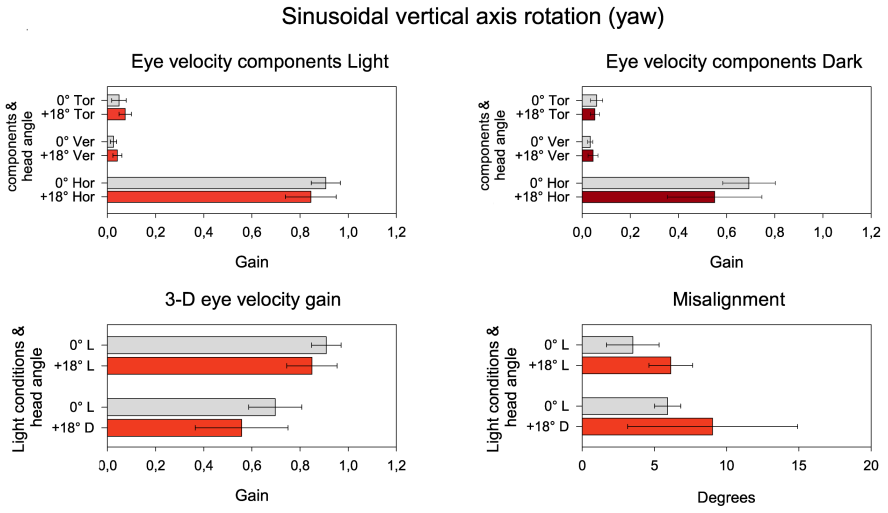

FIGURE C.1: *Eye velocity component results for all tested horizontal stimulus axes averaged over all subjects (N=2) in the light (left), dark (right), and for the head upright (dashed) and pitched up 18° (solid).*

		Torsion		**Vertical**		**Horizontal**	
Rot. ax	*Angle*	*Mean*	*SD*	*Mean*	*SD*	*Mean*	*SD*
-90°	0°	0.05	0.02	0.95	0.11	0.02	0.01
	+18°	0.04	0.02	0.89	0.09	0.03	0.02
−67.5°	0°	0.18	0.03	0.89	0.02	0.04	0.01
	+18°	0.15	0.02	0.84	0.03	0.03	0.00
−45°	0°	0.35	0.06	0.65	0.02	0.05	0.02
	+18°	0.26	0.04	0.60	0.02	0.04	0.01
−22.5°	0°	0.47	0.07	0.32	0.04	0.05	0.02
	+18°	0.35	0.03	0.30	0.03	0.06	0.02
0°	0°	0.43	0.01	0.07	0.02	0.06	0.02
	+18°	0.38	0.04	0.07	0.02	0.05	0.02
22.5°	0°	0.39	0.01	0.42	0.05	0.05	0.01
	+18°	0.34	0.04	0.41	0.06	0.04	0.01
45°	0°	0.32	0.02	0.74	0.04	0.04	0.01
	+18°	0.33	0.01	0.72	0.07	0.02	0.01
67.5°	0°	0.19	0.03	0.93	0.03	0.03	0.01
	+18°	0.19	0.05	0.87	0.10	0.03	0.01
90°	0°	0.05	0.02	0.95	0.11	0.02	0.01
	+18°	0.04	0.02	0.89	0.09	0.03	0.02

TABLE C.1: ***Light:*** *Mean component gains and standard deviations during sinusoidal rotation around axes in the horizontal plane with the head upright (0°) versus pitched up 18° (n=3).*

		Torsion		**Vertical**		**Horizontal**	
Rot. ax	*Angle*	*Mean*	*SD*	*Mean*	*SD*	*Mean*	*SD*
-90°	0°	0.04	0.03	0.84	0.03	0.10	0.06
	+18°	0.06	0.02	0.73	0.11	0.09	0.07
−67.5°	0°	0.18	0.06	0.78	0.01	0.06	0.04
	+18°	0.13	0.03	0.72	0.04	0.04	0.02
−45°	0°	0.31	0.03	0.52	0.02	0.03	0.01
	+18°	0.27	0.03	0.51	0.03	0.06	0.03
−22.5°	0°	0.34	0.07	0.28	0.06	0.12	0.05
	+18°	0.32	0.04	0.24	0.04	0.08	0.06
0°	0°	0.36	0.05	0.08	0.01	0.07	0.05
	+18°	0.32	0.05	0.04	0.01	0.03	0.01
22.5°	0°	0.33	0.08	0.37	0.06	0.06	0.06
	+18°	0.30	0.06	0.35	0.07	0.09	0.05
45°	0°	0.29	0.04	0.67	0.06	0.04	0.02
	+18°	0.26	0.04	0.58	0.08	0.05	0.01
67.5°	0°	0.14	0.03	0.80	0.08	0.05	0.03
	+18°	0.16	0.03	0.74	0.07	0.04	0.03
90°	0°	0.04	0.03	0.84	0.03	0.10	0.06
	+18°	0.06	0.02	0.73	0.11	0.09	0.07

TABLE C.2: ***Dark:*** *Mean component gains and standard deviations during sinusoidal rotation around axes in the horizontal plane with the head upright (0°) versus pitched up 18° (n=3).*

C.2 Transient Stimulation

The effect of the head pitched upwards by 18° compared to the head upright was measured in two subjects for transient stimulation. During stimulation around the vertical axis, the

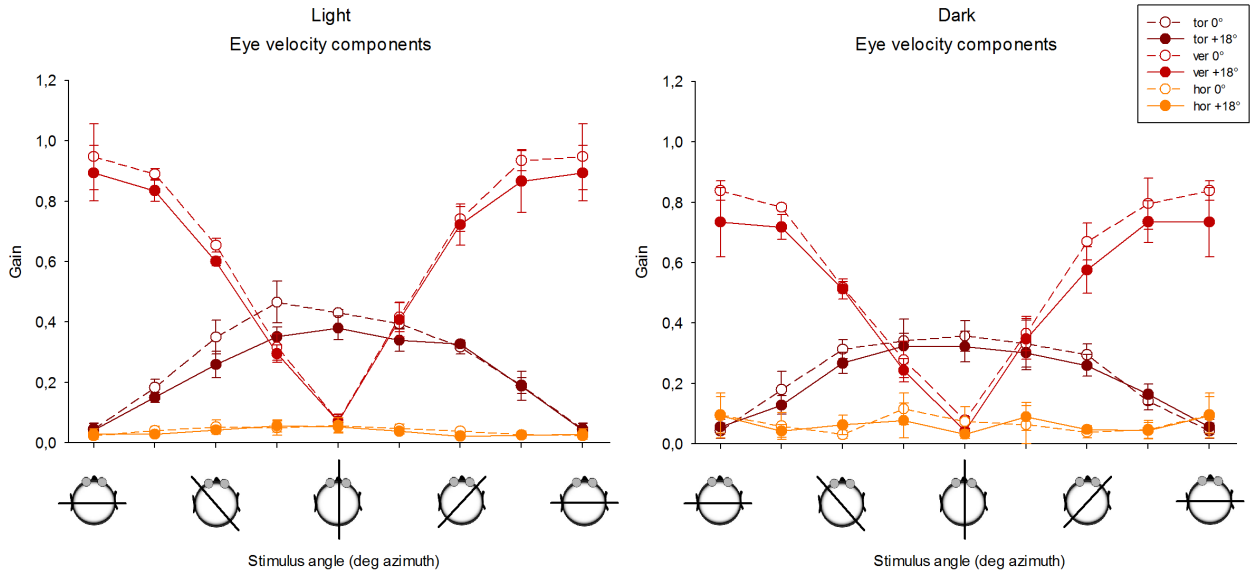

FIGURE C.2: *Eye velocity component results for all tested horizontal stimulus axes averaged over all subjects (N=2) in the light (left), dark (right), and for the head upright (dashed) and pitched up 18° (solid).*

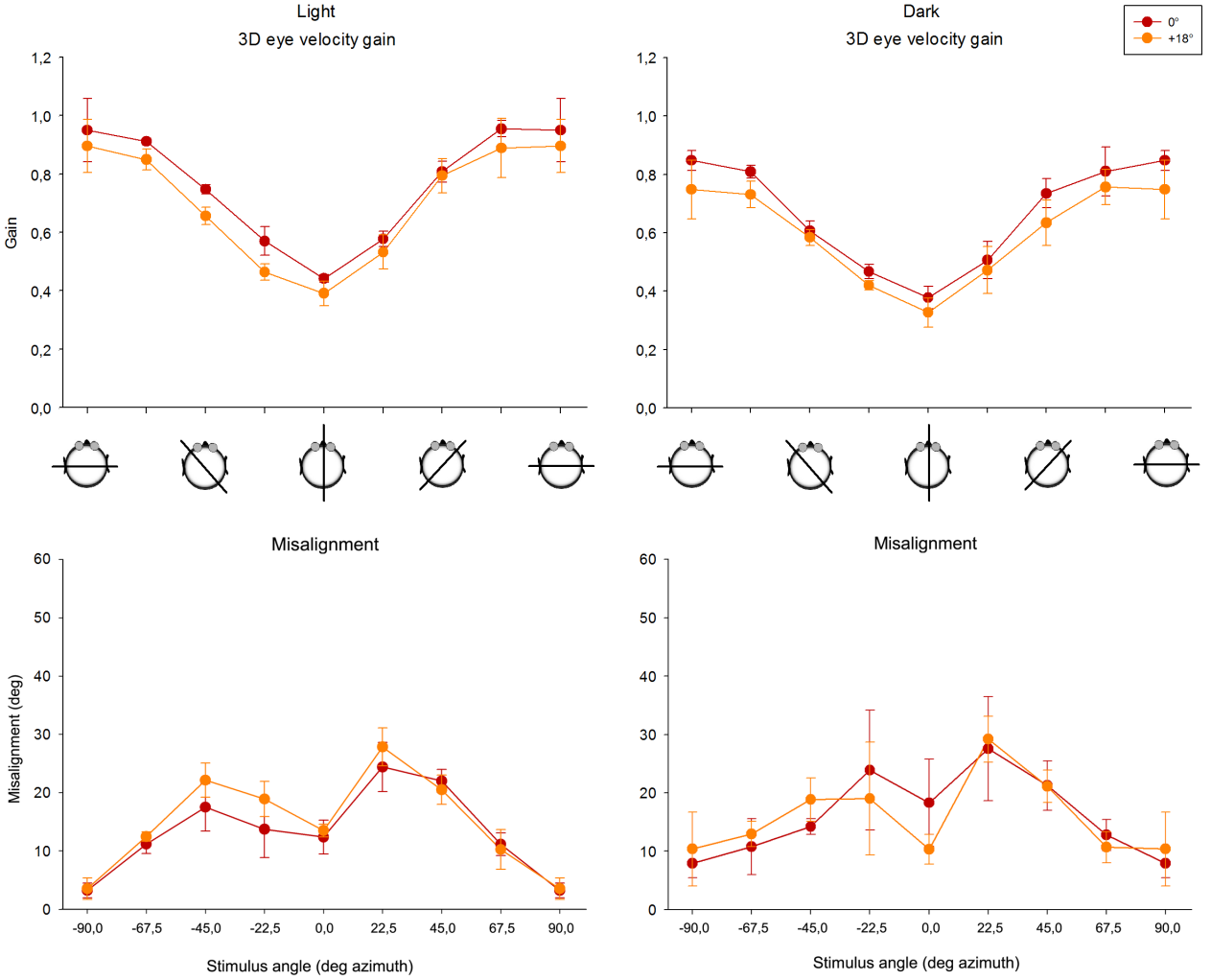

FIGURE C.3: *Eye velocity component results for all tested horizontal stimulus axes averaged over all subjects (N=2) in the light (left), dark (right), and for the head upright (dashed) and pitched up 18° (solid).*

vertical component gain remained unchanged for both the head upright and pitched up, while the horizontal component gain decreased for both rotation directions. For stimulation around axes in the horizontal plane, the vertical component gain was lower with the head pitched up during CW rotation, and was unchanged during CCW rotation. The horizontal component gain was higher for pitch and lower for roll for the head pitched up during CW rotation, while the difference from head upright during CCW rotation was minimal.

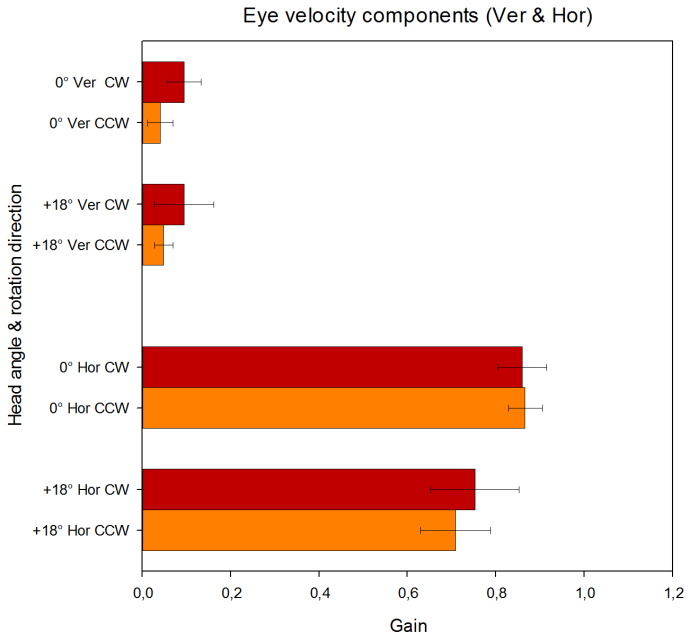

FIGURE C.4: *Horizontal and vertical eye velocity component results for yaw transients in both rotation directions averaged over all subjects (N=5) for the head upright and pitched up 18°.*

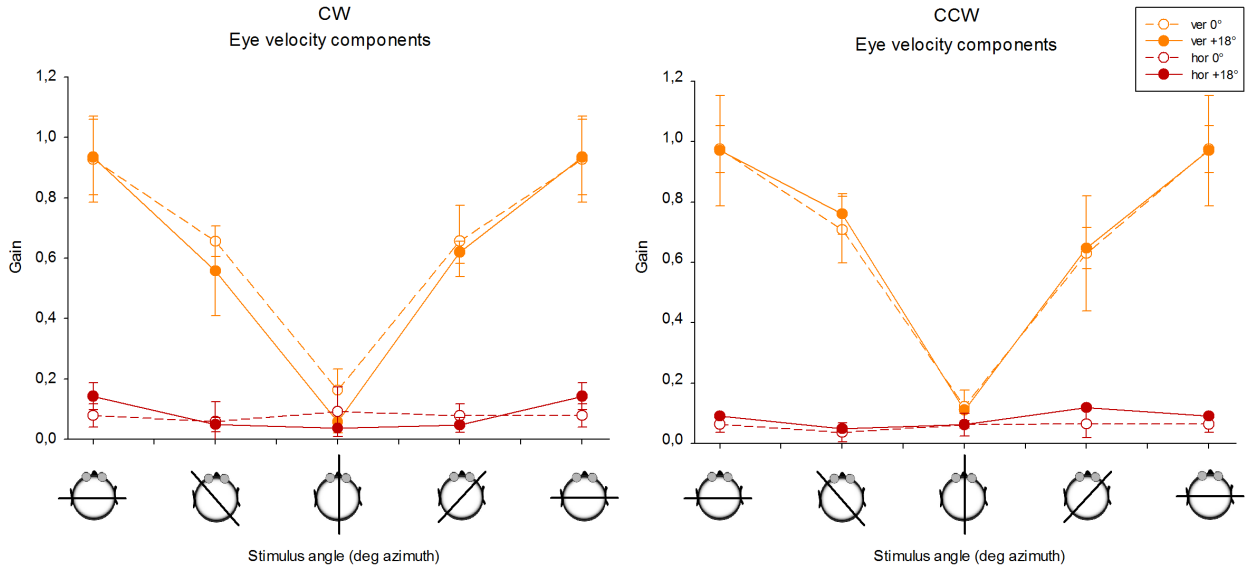

FIGURE C.5: *Eye velocity component results for all tested horizontal stimulus axes averaged over all subjects (N=5) for clockwise (left), counterclockwise (right), and for the head upright (dashed) and pitched up 18° (solid).*

Appendix D

Transients

Persistently deviant data for the torsion component (and thus misalignment and vector gain) after numerous tries to solve the problem within the code, led us to suspect that the culprit could be in the hardware itself. Observing the velocity plots (see Figure D.1) of the dummy coil data, the torsion component trace differs from the vertical and horizontal components in that it is significantly more noisy. After applying the gaussian filter, an oscillation with a frequency of approximately 18 Hz seems to appear. This oscillation can not be attributed to field instability, nor would the dummy coil test setup allow vibrations to be transmitted to the dummy coils. Also, the oscillation would not be limited to just one direction in these cases.

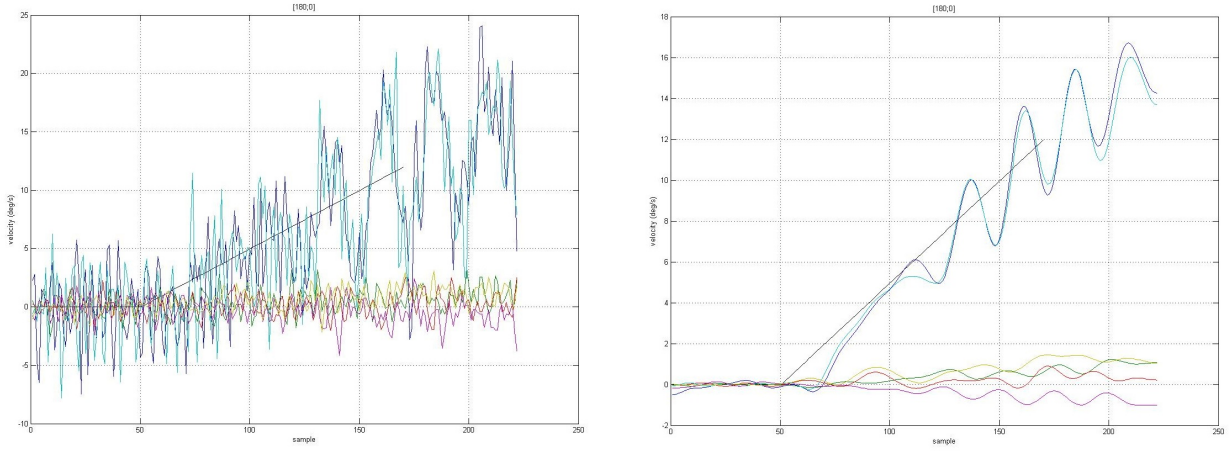

FIGURE D.1: *Velocity plot for CCW transient around roll axis. Torsion is given by the blue-hued lines. The figure on the left shows the raw, noisy traces, a gaussian filter is applied on the right.*

Consequently, included and analyzed in the main body of this report is exclusively the data for the vertical and horizontal components. Shown below are all the plots made before the realization, which thus include the erroneous torsion, misalignment and vector gain

data. Most notably the unreasonably high torsion gains during yaw rotation, the dip in the torsion gain during clockwise roll rotation and the resulting high misalignment stood out as strongly inconsistent with the expectations.

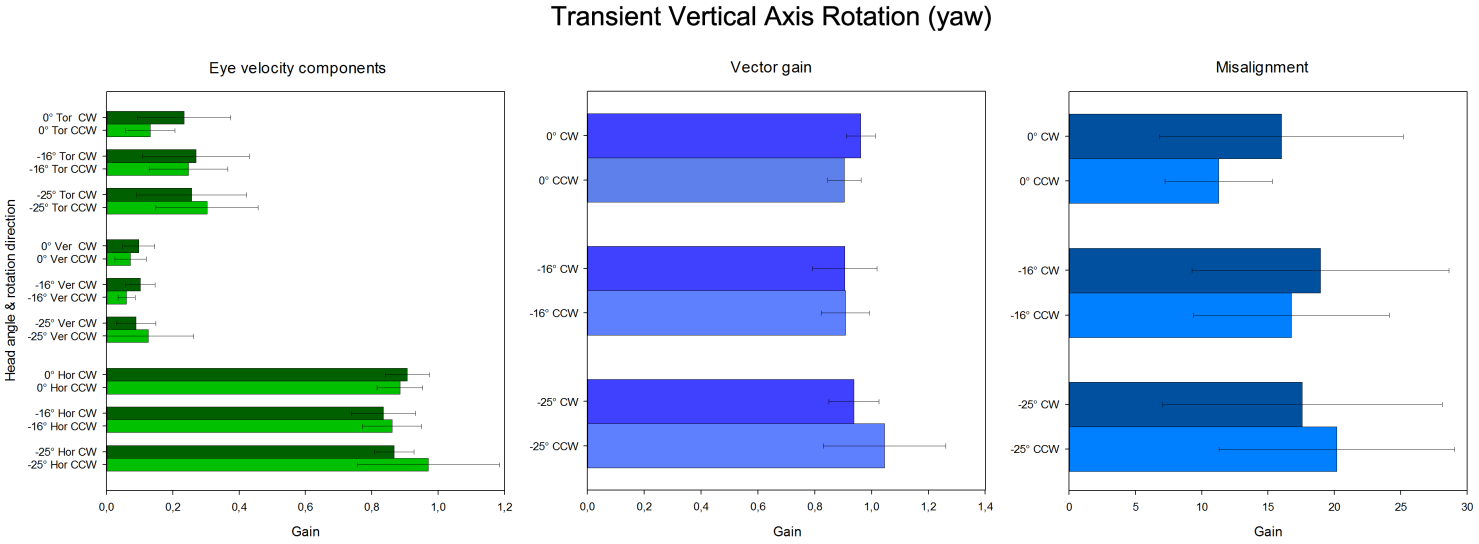

FIGURE D.2: *Eye velocity component results for all tested horizontal stimulus axes averaged over all subjects (N=6) in the light, dark, and for the three head orientations.*

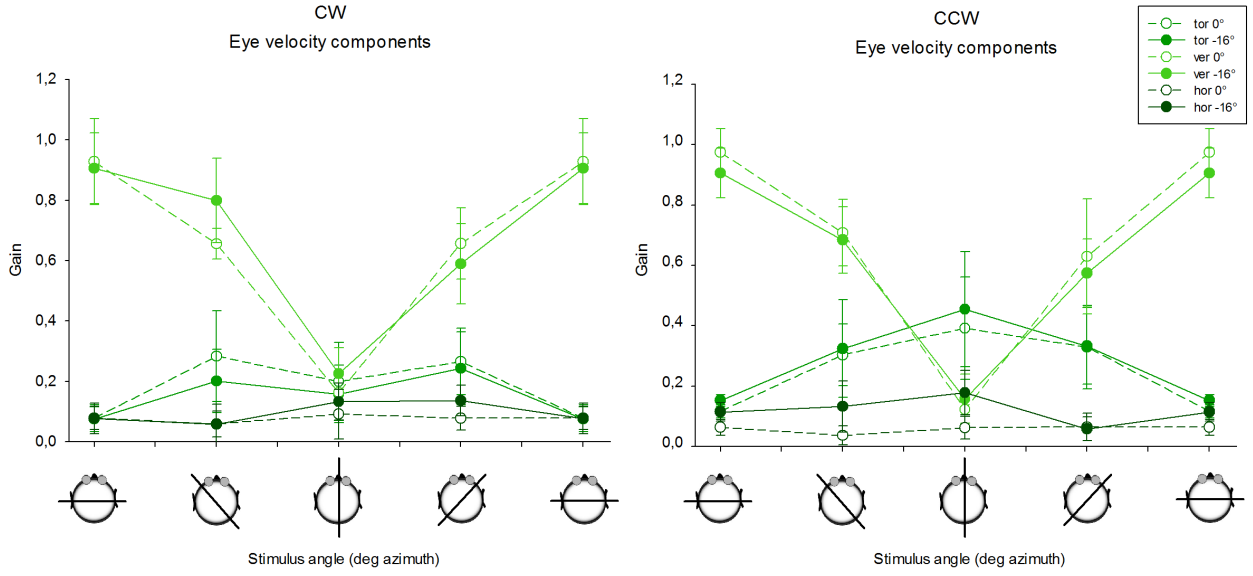

FIGURE D.3: *Eye velocity component results for all tested horizontal stimulus axes averaged over all subjects (N=6) in the light, dark, and for the three head orientations.*

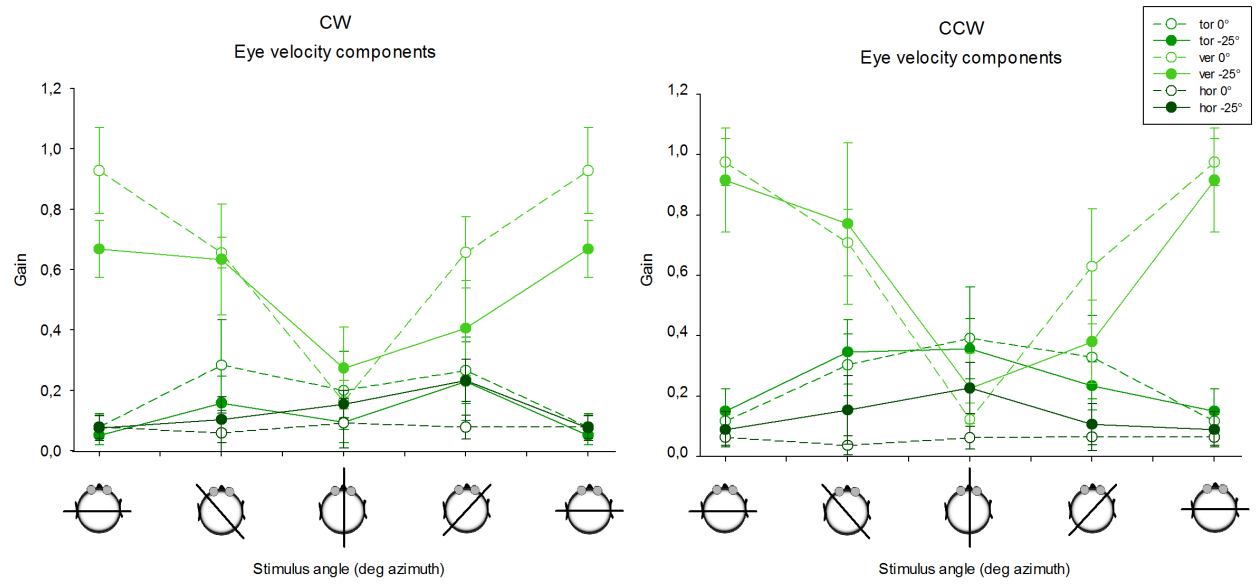

FIGURE D.4: *Eye velocity component results for all tested horizontal stimulus axes averaged over all subjects (N=6) in the light, dark, and for the three head orientations.*

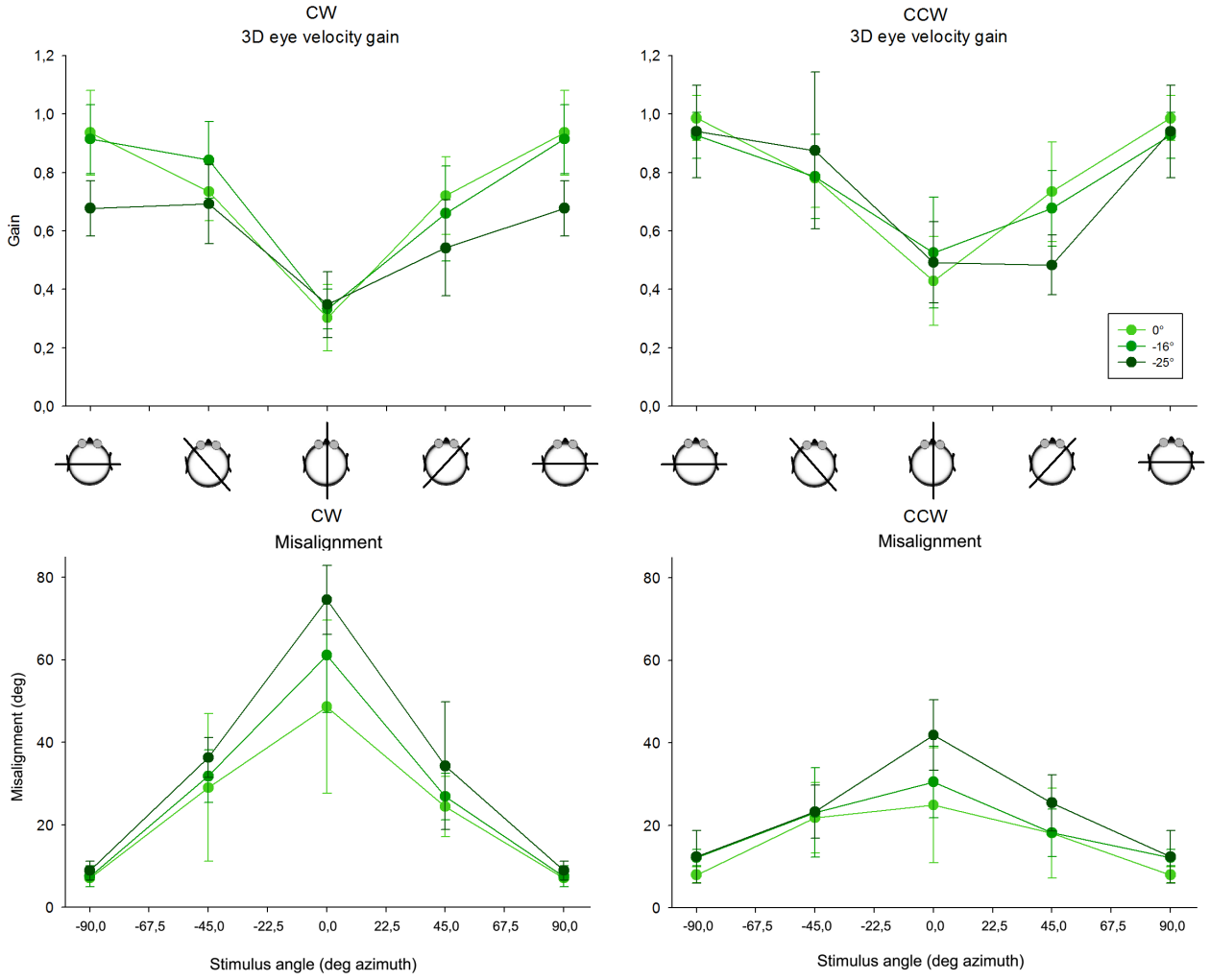

FIGURE D.5: *Eye velocity component results for all tested horizontal stimulus axes averaged over all subjects (N=6) in the light, dark, and for the three head orientations.*

Bibliography

[1] T. Haslwanter, D. Straumann, B.J.M. Hess, and V. Henn. Static roll and pitch in the monkey: shift and rotation of listing's plane. *Vision research*, 32(7):1341–1348, 1992.

[2] R.J. Leigh and D.S. Zee. *"The Neurology of Eye Movements: Fourth Edition"*. Oxford University Press, New York, 2006.

[3] Curthoys I.S. Blanks, R.H.I. and C.H. Markham. Planar Relationships of the Semicircular Canals in Man. *Acta Otolaryngol*, pages 185–196, 1975.

[4] G.R. De Beer. Presidential address: How animals hold their heads. In *Proceedings of the Linnean Society of London*, volume 159, pages 125–139. Wiley Online Library, 1947.

[5] M. Ifediba, S.M. Rajguru, T.E. Hullar, and R.D. Rabbitt. The role of 3-canal biomechanics in angular motion transduction by the human vestibular labyrinth. *Annals of biomedical engineering*, 35(7):1247–63, July 2007.

[6] A.P. Bradshaw, I.S. Curthoys, M.J. Todd, J.S. Magnussen, D.S. Taubman, S.T. Aw, and G.M. Halmagyi. A mathematical model of human semicircular canal geometry: a new basis for interpreting vestibular physiology. *Journal of the Association for Research in Otolaryngology : JARO*, 11(2):145–59, June 2010.

[7] R.D. Rabbitt. Directional coding of three-dimensional movements by the vestibular semicircular canals. *Biological cybernetics*, 80(6):417–31, June 1999.

[8] P.G. Cox and N. Jeffery. Geometry of the semicircular canals and extraocular muscles in rodents, lagomorphs, felids and modern humans. *Journal of anatomy*, 213(5):583–96, November 2008.

[9] A. Haque, D.E. Angelaki, and J.D. Dickman. Spatial tuning and dynamics of vestibular semicircular canal afferents in rhesus monkeys. *Experimental brain research. Experimentelle Hirnforschung. Expérimentation cérébrale*, 155(1):81–90, March 2004.

[10] C.C. Della Santina, V. Potyagaylo, A. Migliaccio, L.B. Minor, and J.P. Carey. Orientation of human semicircular canals measured by three-dimensional multiplanar CT

reconstruction. *Journal of the Association for Research in Otolaryngology : JARO*, 6(3):191–206, September 2005.

[11] J. Marugán-Lobón, L.M. Chiappe, and A.A. Farke. The variability of inner ear orientation in saurischian dinosaurs: testing the use of semicircular canals as a reference system for comparative anatomy. *PeerJ*, 1:e124, January 2013.

[12] L. Girard. Le plan des canaux semi-circulaires horizontaux considéré comme plan horizontal de la tête. *Bulletin et Mémoires de la Societe dAnthropologie de Paris*, (IV):14–33, 1923.

[13] J. Goumans, M.M.J. Houben, J. Dits, and J. van der Steen. Peaks and troughs of three-dimensional vestibulo-ocular reflex in humans. *Journal of the Association for Research in Otolaryngology : JARO*, 11(3):383–93, September 2010.

[14] H. Ichijo. Cupulolithiasis of the horizontal semicircular canal. *European archives of oto-rhino-laryngology : official journal of the European Federation of Oto-Rhino-Laryngological Societies (EUFOS) : affiliated with the German Society for Oto-Rhino-Laryngology - Head and Neck Surgery*, 269(1):53–6, January 2012.

[15] T.D.M. Roberts. *Neurophysiology of postural mechanisms*. Number 66. Butterworths London, 1967.

[16] Team Eyeseecam. EyeSeeCam User Manual. 2013.

[17] Y. Agrawal, M. Davalos-Bichara, M.G. Zuniga, and J.P. Carey. Head Impulse Test Abnormalities and Influence on Gait Speed and Falls in Older Individuals. *Otology & neurotology : official publication of the American Otological Society, American Neurotology Society [and] European Academy of Otology and Neurotology*, August 2013.

[18] B.T. Crane and J.L. Demer. Human Gaze Stabilization During Natural Activities : Translation , Rotation , Magnification , and Target Distance Effects Human Gaze Stabilization During Natural Activities : Translation, Rotation, Magnification, and Target Distance Effects. pages 2129–2144, 2012.

[19] C.C. Della Santina, P.D. Cremer, J.P. Carey, and L.B. Minor. Comparison of head thrust test with head autorotation test reveals that the vestibulo-ocular reflex is enhanced during voluntary head movements. *Archives of otolaryngology–head & neck surgery*, 128(9):1044–54, September 2002.

[20] S.T. Aw, T. Haslwanter, G.M. Halmagyi, I.S. Curthoys, R. a Yavor, and M. J. Todd. Three-dimensional vector analysis of the human vestibuloocular reflex in response to high-acceleration head rotations. I. Responses in normal subjects. *Journal of neurophysiology*, 76(6):4009–20, December 1996.

[21] S. Tabak, H. Collewijn, L.J. Boumans, and J. Steen. van der (1997a) gain and delay of human vestibulo-ocular reflexes to oscillation and steps of the head by a reactive torque helmet. i. normal subjects. *Acta Otolaryngol*, 117:785–795.

[22] S. Tabak, H. Collewijn, L.J. Boumans, and J. Steen. van der (1997b) gain and delay of human vestibulo-ocular reflexes to oscillation and steps of the head by a reactive torque helmet. ii. vestibular-deficient subjects. *Acta Otolaryngol*, 117:796–809.

[23] S.H. Seidman, L. Telford, and G.D. Paige. Vertical, horizontal, and torsional eye movement responses to head roll in the squirrel monkey. *Experimental Brain Research*, pages 218–226, 1995.

[24] M. Fetter, T.C. Hain, and D.S. Zee. Influence of eye and head position on the vestibulo-ocular reflex. *Experimental brain research. Experimentelle Hirnforschung. Expérimentation cérébrale*, 64:208–16, 1986.

[25] D. Anastasopoulos and E. Anagnostou. Invariance of vestibulo-ocular reflex gain to head impulses in pitch at different initial eye-in-orbit elevations: Implications for Alexander's law. *Acta Oto-laryngologica*, 132(January):1066–1072, 2012.

[26] C.J. Bockisch, D. Straumann, and T. Haslwanter. Human 3-D aVOR with and without otolith stimulation. *Experimental brain research. Experimentelle Hirnforschung. Expérimentation cérébrale*, 161(3):358–67, March 2005.

[27] D.E. Angelaki and K.E. Cullen. Vestibular System : The Many Facets of a Multimodal Sense.

[28] D.L. Tomko and G.D. Paige. Linear vestibuloocular reflex during motion along axes between nasooccipital and interaural. *Annals of the New York Academy of Sciences*, 656:233–41, May 1992.

[29] A.H. Clarke, K. Just, W. Krzok, and U. Schönfeld. Listing's plane and the 3D-VOR in microgravity-The role of the otolith afferences. *Journal of Vestibular Research: Equilibrium and Orientation*, 23(2):61–70, 2013.

[30] J.D. Crawford and T. Vilis. Axes of eye rotation and Listing's law during rotations of the head. pages 407–423, 2012.

[31] K. Hepp. On listing's law. *Communications in Mathematical Physics*, 132(1):285–292, 1990.

[32] R.G. Kaptein and J.A.M. Van Gisbergen. Canal and otolith contributions to visual orientation constancy during sinusoidal roll rotation. *Journal of neurophysiology*, 95(3):1936–1948, 2006.

[33] J.P. Carey and C.C. Della Santina. Principles of Applied Vestibular Physiology. 2009.

[34] D. Tweed, D. Sievering, H. Misslisch, M. Fetter, D. Zee, and E. Koenig. Rotational kinematics of the human vestibuloocular reflex. i. gain matrices. *Journal of neurophysiology*, 72(5):2467–2479, 1994.